Published in final edited form as:
Sci Signal. 2011 September 27; 4(192): ra64. doi:10.1126/scisignal.2002049.

Tyrosine Phosphorylation of the Guanine Nucleotide Exchange Factor GIV Promotes Activation of PI3K During Cell Migration

Changsheng Lin[1], **Jason Ear**[1], **Yelena Pavlova**[1], **Yash Mittal**[1], **Irina Kufareva**[4], **Majid Ghassemian**[3], **Ruben Abagyan**[4], **Mikel Garcia-Marcos**[2], and **Pradipta Ghosh**[1,§]

[1]Department of Medicine, University of California, San Diego, School of Medicine, La Jolla, California, 92093.

[2]Department of Cellular and Molecular Medicine, University of California, San Diego, School of Medicine, La Jolla, California, 92093.

[3] Departments of Chemistry and Biochemistry, University of California, San Diego, School of Medicine La Jolla, California, 92093.

[4]School of Pharmacy/Pharmaceutical Sciences, University of California, San Diego, La Jolla, California, 92093.

Abstract

GIV (Gα-interacting vesicle-associated protein; also known as Girdin), enhances Akt activation downstream of multiple growth factor– and G-protein–coupled receptors to trigger cell migration and cancer invasion. Here we demonstrate that GIV is a tyrosine phosphoprotein that directly binds to and activates phosphoinositide 3-kinase (PI3K). Upon ligand stimulation of various receptors, GIV was phosphorylated at Tyr^{1764} and Tyr^{1798} by both receptor and non-receptor tyrosine kinases. These phosphorylation events enabled direct binding of GIV to the N- and C-terminal SH2 domains of p85α, a regulatory subunit of PI3K, stabilized receptor association with PI3K, and enhanced PI3K activity at the plasma membrane to trigger cell migration. Tyrosine phosphorylation of GIV and its association with p85α increased during metastatic progression of a breast carcinoma. These results suggest a mechanism by which multiple receptors activate PI3K through tyrosine phosphorylation of GIV, thereby making the GIVPI3K interaction a potential therapeutic target within the PI3K-Akt pathway.

INTRODUCTION

GIV (Gα-interacting vesicle-associated protein; also known as girdin), is a multi-domain protein which is required for growth factors (EGF (1, 2), IGF (3), VEGF (4), and insulin (5-8)) to enhance Akt activation in a PI3K-dependent manner (5), remodel actin and trigger cell migration. GIV also enhances Akt activation downstream of G-protein coupled

[§]**To whom correspondence should be addressed.** Telephone: 858-822-7633. Fax: 858-822-7636. prghosh@ucsd.edu..

Author contributions: C.L., J.E., Y.P., Y.M., M.G-M., and P.G. performed experiments. I.K. and R.A. performed computational modeling. M.G. performed the mass spectrometry studies. Y.P., C.L., and J.E. prepared and characterized the protein constructs. C.L., J.E., Y.M., M.G-M and P.G. designed the experiments and analyzed the data. C.L., M.G-M., and P.G. wrote the paper.

Competing interests: None to declare.

receptors (GPCRs) (7-9). Working downstream of growth factor receptor tyrosine kinases and GPCRs, GIV enhances Akt signals during diverse biological processes, including epithelial wound healing, macrophage chemotaxis, development, autophagy, tumor angiogenesis, tumor cell migration, and cancer invasion and metastasis (1-4, 6-9).

We previously demonstrated that GIV is a non-receptor guanine-nucleotide exchange factor (GEF) for Gαi (7) and that GIV directly binds ligand-activated epidermal growth factor receptor (EGFR) (2). By linking G protein signaling to EGFR and assembling a Gαi-GIV-EGFR signaling complex, GIV enhances EGFR autophosphorylation, prolongs receptor association with the plasma membrane, and enhances Akt signals from the plasma membrane (PM) to trigger cell migration. However, the underlying mechanism of how multiple receptors utilize GIV for Akt-enhancement has remained unknown.

Because tyrosine phosphorylation-based signaling pathways are major activators of the PI3K-Akt pathway and because GIV responds to multiple growth factor receptor tyrosine kinases to enhance Akt activation in a PI3K-dependent manner (5), we investigated whether GIV is a substrate for tyrosine kinases and whether such phosphorylation would regulate its ability to activate PI3K.

RESULTS

GIV is phosphorylated by receptor and non-receptor tyrosine kinases

To investigate whether GIV is phosphorylated by tyrosine kinases we performed in vitro kinase assays using recombinant growth factor receptor tyrosine kinases (EGFR, PDGFR, and VEGFR) and the C-terminal domain of GIV (His-GIV-CT; aa 1660-1870) and determined the extent of GIV phosphorylation by immunoblotting for phosphotyrosine. We examined the C-terminus of GIV because GIV directly binds EGFR through this domain (2). All three receptor tyrosine kinases phosphorylated GIV to a similar extent (**Fig 1A**), as did TrkA, the receptor for nerve growth factor (NGF) (**Fig S1A**). Similar results were obtained when the C-terminal domain of His-GIV was subjected to kinase assays with recombinant c-Src, a non-receptor tyrosine kinase (**Fig 1A**). To determine whether GIV was tyrosine phosphorylated in cells, we immunoprecipitated endogenous GIV from EGF-treated HeLa cells and immunoblotted for phosphotyrosine and GIV, and found that GIV was phosphorylated on tyrosine residues in cells treated with EGF (**Fig 1B,** lanes 1-2). When tyrosine phosphoproteins were immunoprecipitated from HeLa cells using a phosphotyrosine antibody, GIV was detected in the immunoprecipitates (**Fig 1B,** lanes 3-4), thus confirming that GIV is a tyrosine phosphoprotein in cells treated with EGF. Similar results were also observed in HeLa cells after insulin stimulation (**Fig S1B**). We conclude that GIV is a tyrosine phosphoprotein that is a common target of receptor and non-receptor tyrosine kinases.

We performed mass spectrometry on in vitro EGFR-phosphorylated C-terminal domain of GIV and identified Tyr^{1764} and Tyr^{1798} as the sites of phosphorylation (**Fig 1C**, **Fig S2**). A phylogenetic analysis of GIV revealed that these two tyrosine residues are conserved in birds and mammals, whereas both are absent in fish or lower animals (**Fig S2D**). These tyrosine residues were previously identified as major phosphosites in cells

(www.Phosphosite.org) based on the curated information from several independently-conducted, high-throughput phosphoproteomic studies (10-14) (**Fig S2A**). In addition, multiple kinase prediction programs identified the sequences flanking these tyrosine residues as suitable substrates for both receptor and non-receptor tyrosine kinases (**Fig S2A**). Whereas the sequence flanking Tyr^{1764} was predicted to make that site favorable for EGFR, the sequence flanking Tyr^{1798} appeared favorable for Src (**Fig S2B, C**). In vitro kinase assays using the C-terminal domain of GIV with phenylalanine substitutions for either or both of the tyrosine residues confirmed that both Tyr^{1764} and Tyr^{1798} were substrates for EGFR and Src (**Fig 1D**). The $Tyr^{1798}\rightarrow$Phe (Y1798F) mutant was a better substrate for EGFR, whereas the $Tyr^{1764}\rightarrow$Phe (Y1764F) mutant was a better substrate for Src. Because both kinases failed to phosphorylate the mutant lacking both tyrosine residues, we conclude that these residues accounted for the observed in vitro phosphorylation (Fig. **1A**). To discern if these two C-terminal tyrosine residues also account for the phosphorylation of full length GIV observed in cells in Fig. **1B**, we determined the tyrosine phosphorylation status of wild-type GIV (GIV-WT) or a GIV mutant in which both tyrosine residues were replaced by phenylalanines (GIV-YF) in Cos7 cells. Upon EGF stimulation, wild-type GIV, but not the tyrosine phosphorylation deficient mutant, was tyrosine phosphorylated (**Fig 1E**), suggesting that Tyr^{1764} and Tyr^{1798} may be the major sites of tyrosine phosphorylation in GIV. Taken together, these results demonstrate that both EGFR and Src can phosphorylate GIV at two C-terminally located tyrosine residues in vitro, and that these residues are phosphorylated after ligand stimulation in cells.

Receptor and non-receptor tyrosine kinases cooperatively phosphorylate GIV after stimulation of receptor tyrosine kinases and GPCRs

Because EGF stimulation results in activation of both EGFR and Src (15), we asked whether ligand-dependent tyrosine phosphorylation of GIV is mediated by both receptor and non-receptor kinases. We used a selective inhibitor for Src family kinases, PP2 (16), in cellular phosphorylation assays. Upon EGF stimulation, wild-type GIV was phosphorylated in the presence and absence of PP2 (**Fig S3**), suggesting that GIV is tyrosine phosphorylated, likely by EGFR, when Src family kinases are inhibited. Because ligand-stimulation of GPCRs also activates Src (17), we asked if activation of G-protein coupled receptors (GPCRs) of the lysophosphatidic acid (LPA) family also triggered tyrosine phosphorylation of GIV. LPA stimulation resulted in the phosphorylation of wild-type GIV, but not the tyrosine phosphorylation deficient mutant (**Fig 1F**), indicating that Tyr^{1764} and Tyr^{1798} account for the observed tyrosine phosphorylation of GIV after LPA treatment. Phosphorylation of wild-type GIV was attenuated when cells were incubated with PP2 prior to LPA stimulation, indicating that ligand-stimulation of the LPA receptor triggers tyrosine phosphorylation of GIV through Src family kinases. Collectively these results demonstrate that both EGF and LPA trigger tyrosine phosphorylation of GIV: EGF triggers phosphorylation by EGFR, whereas LPA primarily utilizes non-receptor tyrosine kinases like the Src kinase family to phosphorylate GIV. We conclude that both receptor and non-receptor kinases can phosphorylate GIV in cells after ligand stimulation.

Tyrosine phosphorylation of GIV is required for enhancement of Akt phosphorylation, actin remodeling and for cell migration

To investigate whether tyrosine phosphorylation is required for GIV's functions, such as enhancement of Akt activation, actin remodeling and cell migration (18), we generated HeLa cell lines that were depleted of endogenous GIV by siRNA (7) and that stably expressed an siRNA-resistant but otherwise wild-type form of GIV (HeLa-GIV-WT) or an siRNA-resistant form of GIV that could not be tyrosine phosphorylated (HeLa-GIV-YF) at an abundance ~1.5-2 fold above that of endogenous GIV. In cells expressing the tyrosine phosphorylation GIV mutant and in GIV-depleted HeLa cells, phosphorylation of Akt was reduced compared to that in cells expressing wild-type GIV (**Fig 2A**). Furthermore, cells expressing the tyrosine phosphorylation GIV mutant showed impaired formation of actin stress fibers and inefficient migration in scratch-wound assays (**Fig 2, B and C**). Cells expressing a GIV mutant lacking a functional GEF motif ($Phe^{1685}\rightarrow Ala$) that cannot interact with or activate Gαi (7) fail to remodel actin, enhance Akt phosphorylation, or migrate after scratch-wounding (19). Akt phosphorylation was reduced to a greater extent in cells expressing the phosphorylation-deficient GIV mutant than in cells expressing the GIV mutant lacking the GEF motif (**Fig 2D**). Regardless, expression of the tyrosine phosphorylation deficient mutant (in HeLa-GIV-YF cells) or the mutant lacking a functional GEF motif (in HeLa-GIV-FA cells) did not rescue the functions of GIV when endogenous GIV was depleted (**Fig 2B-D**), indicating that both tyrosine phosphorylation of GIV and its GEF function are required for regulating Akt signaling and actin remodeling during cell migration.

The phosphotyrosines of GIV function independently of its GEF motif

We sought to determine whether tyrosine phosphorylation affects the ability of GIV ability to bind and activate Gαi3. Both mock-treated and phosphorylated GIV C-terminal fragments bound Gαi3 to a similar extent in pulldown assays (**Fig 2E**) and activated Gαi3, as assessed by the steady-state GTPase activity of the G protein, in a dose-dependent manner and with similar potencies (**Fig 2F**). Furthermore, both GIV C-terminal fragments increased the GTPase activity of Gαi3 by ~1.7-fold over the basal activity at 0.6 μM, the highest concentration of GIV C-terminus protein tested. Thus, tyrosine phosphorylation of GIV does not affect the Gαi3-GIV interaction or the GEF activity of GIV towards Gαi3.

We next wanted to determine whether the GEF function of GIV was required for tyrosine phosphorylation of GIV. The GIV C-terminal fragment with the GEF motif mutation was phosphorylated to a similar extent as wild-type by EGFR in in vitro assays **(Fig S4A)** and in EGF-treated HeLa cells (**Fig S4B**), indicating that the GEF function was not required for tyrosine phosphorylation of GIV in cells. Thus, tyrosine phosphorylation and the GEF motif of GIV function independently of each other during cell migration.

Tyrosine phosphorylated GIV binds the SH2 domains of p85α

Tyrosine signaling pathways have been implicated in the activation of class I PI3Ks through direct binding to the SH2 domains of the p85α regulatory subunit of PI3Ks or indirect binding to other SH2 domain-containing proteins and adaptors (20). To investigate whether tyrosine phosphorylated GIV binds to SH2 domain containing proteins, we performed pull-

down assays using sham-treated or in vitro EGFR-phosphorylated His-GIV C-terminal fragments with a panel of SH2 adaptors. We used this approach because essential features of specific interactions between phosphoproteins and SH2-containing proteins can be reconstituted with phosphopeptides and SH2 domain fragments (21). Phosphorylated, but not sham-treated GIV C-terminus, bound to the C-terminal SH2 domain of p85α (p85α-CSH2) and to a lesser extent to the N-terminal SH2 domain of p85α (p85α-NSH2) (**Fig 3A**), but not to other SH2 domains (c-Src, Gab1, or Grb2). Phosphorylation of GIV C-terminus by EGFR or Src enabled binding to the C-terminal SH2 domain 7 of p85α (**Fig 3B**), suggesting that both receptor and non-receptor tyrosine kinases can generate phosphotyrosines on the C-terminus of GIV that are recognized by the SH2 domains of p85α. In addition, the C-terminal SH2 domain of p85α bound to more endogenous GIV from EGF-stimulated Cos7 cells than from serum starved cells (**Fig S5A**). Furthermore, endogenous (**Fig 3 C, D**) and exogenously expressed (**Fig S5B**) GIV coimmunoprecipitated with p85α after ligand stimulation of serum starved cells. The formation of endogenous GIV-p85α complexes coincided with the timing of peak tyrosine phosphorylation of GIV and peak Akt activation, all of which occurred at ~5 min after ligand stimulation (**Fig 3C**). Furthermore, the GIV-p85α association occurred after stimulation with any of the ligands tested (**Fig 3D, S5B**), suggesting that assembly of GIV-p85α complexes in cells can be triggered by multiple growth factors. However, the tyrosine phosphorylation deficient GIV mutant coimmunoprecipitated with ligand-activated EGFR, but not with p85α (**Fig 3E**), thereby demonstrating that phosphorylation of Tyr^{1764} and Tyr^{1798} are required for the formation of GIV-p85α complexes in cells, but not for the GIV-EGFR interaction. Based on our findings we conclude that upon ligand stimulation GIV directly binds ligand-activated EGFR and enhances the recruitment of p85α to the activated receptor through binding of the SH2 domains of p85α to its C-terminally located phosphotyrosines.

Homology models reveal similarities between the GIV-p85α interface and canonical phosphotyrosine-SH2 interactions

To determine the relative contribution of Tyr^{1764} and Tyr^{1798} towards the observed interaction between the C-terminus of GIV and the SH2 domains of p85α, we carried out pull-down assays on in vitro phosphorylated wild-type or single tyrosine mutant forms of the GIV C-terminal fragment with the C-terminal SH2 domain of p85α. When EGFR was used to phosphorylate the GIV C-terminal fragments, the C-terminal SH2 domain of p85α bound to wild-type and the Y1798F mutant, but not the Y1764F mutant (**Fig 4A**). By contrast, when Src was used to phosphorylate the GIV C-terminal fragments, the C-terminal SH2 domain of p85α bound to wild-type and the Y1764F mutant, but not the Y1798F mutant (**Fig 4A**). Thus, EGFR triggers binding of GIV to p85α mostly through phosphorylation of Tyr^{1764} and Src does so mostly through phosphorylation of Tyr^{1798} (**Fig 1D**). These results indicate that EGFR and Src create two distinct phosphotyrosine-binding sites on GIV for the C-terminal domain of p85α. In addition, both phosphotyrosines also directly bound to the N-terminal SH2 domain of p85α (**Fig 4B**), indicating that both N- and C-terminal SH2 domains of p85α have the ability to bind either of the two phosphotyrosines on GIV.

Next we aligned GIV's phosphopeptides (pY^{1764}FISS and pY^{1798}ATLP) with phosphotyrosine peptides from other proteins that bind to the C-terminal domain of p85α

(**Fig 4C**) and found that the GIV phosphopeptides do not resemble the canonical consensus sequence for peptides that bind the N- or C-terminal SH2 domains of p85α, pY[VMLI]XM (19). To gain insights into how these non-canonical phosphopeptides of GIV interact with the SH2 domains of p85α. we created the homology models (**Fig 4D, E; Fig S6**) with the Internal Coordinate Mechanics (ICM) software (22, 23) using the crystal structures of the C-terminal SH2 domain of p85 in complex with $pTyr^{751}$ peptide from PDGFRβ (24), or the N-terminal SH2 domain of p85 bound to c-Kit phosphotyrosyl peptide (25) as templates. $pTyr^{1764}$ of GIV makes hydrogen bonds with residues of the C-terminal SH2 in a manner similar to the established crystal structure of this domain with $pTyr^{751}$ of PDGFRβ. Similarly, $pTyr^{1798}$ of GIV makes hydrogen bonds with residues of the N-terminal SH2 domain as seen in the resolved crystal structure of this domain complexed with phosphotyrosyl peptide of c-Kit. The side chains of both phosphotyrosines of GIV make multiple hydrogen bonds with Arg^{631}, Arg^{649}, Ser^{651}, and Ser^{652} of the C-terminal domain of p85α and with Arg^{340}, Arg^{358}, Ser^{361}, Thr^{369}, and Lys^{382} of the N-terminal domain of p85α, whereas the backbones of the phosphopeptides of GIV form hydrogen bonds with His^{669}, His^{706}, and Asn^{707} in the C-terminal domain of p85α and Asn^{378}, Leu^{380}, Asn^{417} in the N-terminal domain of p85α (**Fig 4D,E; Fig S6AD**). Multiple polar and non-polar contacts were also observed between the phosphotyrosine peptides of GIV and the SH2 domains of p85α. For example, Phe^{1765} of GIV-pY^{1764}FISS bound a shallow hydrophobic pocket occupied by Val^{752} of PDGFRβ and Met^{724} of c-Kit in their respective complex structures with the C- and N-terminal SH2 domains of p85α, whereas Leu^{1801} of GIV pY^{1798}ATLP occupies a deep cavity which binds Met^{754} of PDGFRβ and Met^{724} of c-Kit in their respective complex structures with the C- and N-terminal SH2 domains of p85α. These analyses suggest that the sequences flanking both phosphotyrosine peptides of GIV are equally compatible with direct and specific binding to either SH2 domains of p85α (**Fig 4A, B**).

The phosphotyrosines of GIV couple PI3K to ligand-activated receptor tyrosine kinases

Because GIV directly binds ligand-activated EGFR (2) and p85α, we investigated if GIV, and more specifically its phosphotyrosines, facilitate the recruitment of PI3K to activated EGFR. In HeLa cells expressing wild-type GIV, EGFR transiently and maximally associated with p85α at 5 min after ligand stimulation, whereas in cells expressing the tyrosine phosphorylation deficient GIV mutant, p85α recruitment was reduced **(Fig 5A)**. Thus, tyrosine phosphorylation of GIV is critical for effective formation or stabilization of the p85α-EGFR complex. Similar results were obtained with exogenously expressed insulin receptor (**Fig 5B**), suggesting that tyrosine phosphorylation of GIV may also be critical for effective formation or stabilization of a p85α-insulin receptor complex. These results suggest that interactions between receptor tyrosine kinases and p85α in cells are enhanced by GIV through its C-terminal phosphotyrosines.

Tyrosine phosphorylated GIV activates PI3K at the plasma membrane

Binding of phosphotyrosines to both SH2 domains of the regulatory p85α subunit activates the catalytic p110 subunit of PI3K (19, 26) which triggers the production of phosphatidylinositol-3,4,5-trisphosphate (PI-3,4,5P or PIP_3)(27-31). Because phosphotyrosines of GIV directly bind to the SH2 domains of p85α, this interaction would

be expected to activate PI3K. We carried out in vitro PI3K assays (32) using purified phosphoinositides and immunoprecipitated p85α from cells expressing vector, wild-type GIV, or the tyrosine phosphorylation deficient form of GIV. The activity of PI3K, as determined by the extent of production of PI3P, was low in cells expressing vector or the tyrosine phosphorylation deficient form of GIV, and was higher in cells .expressing wild-type GIV (**Fig 5C**), indicating that phosphorylation of Tyr^{1764} and Tyr^{1798} in GIV enhances PI3K activity in cells. To determine if this activation of PI3K occurred at the plasma membrane and whether the abundance of PIP_3 was increased, we expressed the GFP-tagged PH domain of Akt (Akt-PHGFP) (**Fig 5D**), which recognizes PIP_3 (33-35), and monitored its EGF-dependent recruitment to the plasma membrane. In serum-starved HeLa control cells, the Akt-based PIP_3 reporter was mostly cytosolic, but was recruited to the plasma membrane within 10 min after EGF stimulation, indicating activation of PI3K was activated and generation of PIP_3 at the plasma membrane after ligand stimulation. Cells expressing wild-type GIV showed a similar pattern of robust EGF-triggered recruitment of the Akt-based PIP_3 reporter to the plasma membrane. By contrast, in cells expressing the tyrosine phosphorylation deficient form of GIV, the Akt-based PIP_3 reporter remained cytosolic before and after EGF treatment, indicating that the abundance of PIP_3 at the plasma membrane does not change in these cells after ligand stimulation. To circumvent the possibility that altered localization of Akt in cells expressing the tyrosine phosphorylation deficient form of GIV could be due to changes in interaction between GIV and Akt (1, 5), we performed similar assays using a second validated reporter for PIP_3 which contains the PH domain of Bruton's tyrosine kinase (36) (Btk-PH-GFP) (**Fig S7**). Findings with the Btk-based PIP_3 reporter were similar to those with the Akt-based PIP_3 reporter, demonstrating that EGF-triggered production of PIP_3 is impaired in cells expressing the tyrosine phosphorylation deficient form of GIV. We conclude that ligand-stimulated activation of PI3K and production of PIP_3 at the plasma membrane requires tyrosine phosphorylation of GIV.

Tyrosine phosphorylation of GIV and its association with p85α increases during metastatic progression of a breast carcinoma

We previously showed that the abundance of GIV protein and mRNA increases during metastatic progression in colorectal and breast carcinomas (6), an increase that coincides with increased activity of the PI3K-Akt pathway in tumor cells (37, 38). We investigated the extent of tyrosine phosphorylation of GIV and its association with p85α during metastatic progression using 21T series of human mammary cells (16N, NT and MT2) (2). These cells were derived by successive biopsies from a single patient with breast cancer: 16N is from the normal breast, NT from the primary tumor (invasive ductal carcinoma), and MT2 from the metastatic pleural effusions. Consistent with our previous work (2, 9), the abundance of full-length GIV and extent of Akt phosphorylation were lowest in 16N, intermediate in NT and highest in MT2 (**Fig 5E**). Tyrosine phosphorylation of GIV and the amount of p85α that coimmunoprecipitated with GIV were lowest in 16N, intermediate in NT, and highest in MT2 cells (**Fig 5E**). These results suggest that tyrosine phosphorylation of GIV and its association with p85α may increase during metastatic progression of breast carcinoma and suggest that GIV-dependent PI3K activation may play a role during tumor invasion.

Tyrosine phosphorylation of GIV is required for Akt-dependent phosphorylation of GIV at Ser^{1416}

The phosphorylation of GIV at Ser^{1416} by Akt has been attributed to multiple biological functions of GIV, including cancer invasion and metastasis, neoangiogenesis, control of cell size during development, neuronal migration and vascular repair after injury (1-4, 6, 8, 9, 39-42). Thus, we investigated the relationship between tyrosine-phosphorylation and Akt-dependent serine phosphorylation of GIV. Phosphorylation of wild-type GIV at Ser^{1416} was higher than that of the tyrosine phosphorylation-deficient mutant (**Fig 6A**), suggesting that tyrosine phosphorylation of GIV is a prerequisite for efficient Akt-dependent serine phosphorylation of GIV. The serine phosphorylation-deficient Ser^{1416}→Ala (S1416A) and the serine phosphorylation-mimicking Ser^{1416}→Asp (S1416D) mutants of GIV were tyrosine phosphorylated to a similar extent as wild-type GIV (**Fig 6B**), indicating that the phosphorylation status of Ser^{1416} does not affect tyrosine phosphorylation of GIV. Taken together, these findings suggest that tyrosine phosphorylation of GIV occurs upstream of and regulates the subsequent step of Akt-dependent phosphorylation of GIV at Ser^{1416}.

Our results demonstrate that GIV is a substrate of multiple tyrosine kinases and that the phosphotyrosines of GIV directly bind to and activate Akt and PI3K at the plasma membrane (**Fig 6C**). Activated Akt subsequently phosphorylates GIV and triggers cell migration (5, 7, 8). Based on these findings, we propose that multiple receptors enhance PI3K activity and trigger cell migration through a common tyrosine phosphoprotein, GIV.

DISCUSSION

Tyrosine-Phosphorylated GIV Serves as a Common Platform to enhance PI3K activity During Cell Migration

In this work we describe GIV, a non-receptor guanine nucleotide exchange factor for Gαi3, as a key molecule in the tyrosine signaling pathway. We demonstrate that GIV is a common substrate for multiple receptor and non-receptor tyrosine kinases and identify the sites of phosphorylation as Tyr^{1764} and Tyr^{1798} in its C-terminus. These phosphotyrosines are required for GIV to bind to p85α in vitro and for the ligand-dependent formation of GIV-p85α complexes in cells. In HeLa cells expressing wild-type GIV, in which Tyr^{1764} and Tyr^{1798} undergo ligand-dependent phosphorylation, PI3K is activated to generate PIP_3 at the plasma membrane, activation of Akt is enhanced, actin is remodeled and cell migration is triggered. By contrast, HeLa cells expressing a GIV mutant in which both tyrosines are replaced by phenylalanines show defective ligand-dependent activation of PI3K, lack of enhanced Akt activation, absence of actin remodeling, and lack of migration. We conclude that GIV enhances ligand-stimulated PI3K activity via phosphotyrosines in its C-terminus.

We also provide the mechanism for GIV-dependent enhancement of PI3K activity by two diverse classes of chemotactic receptors: growth factor receptor tyrosine kinases and GPCRs. We found that GIV was tyrosine phosphorylated after cells are stimulated with either growth factors like EGF and insulin or with a GPCR ligand like LPA. Upon EGF stimulation GIV was phosphorylated at two particular tyrosine residues by activated EGFR, whereas upon LPA stimulation GIV was phosphorylated at these same residues primarily by

Src family kinases. Tyrosine phosphorylated GIV bound the regulatory p85α subunit of PI3K. Thus, tyrosine phosphorylation of GIV and the formation of GIV-p85α complexes are triggered by multiple receptors that require GIV to enhance Akt signals (2, 6-8, 43). We conclude that the tyrosine kinase-phosphoGIV-p85α-axis serves as a common pathway initiated by multiple receptors to enhance PI3K activity during cell migration.

Previous work has established that migrating cells display a steep PI3K-Akt signaling gradient that is restricted to the leading edge (34, 44). However, the uniformity of distribution of chemotactic receptors (receptor tyrosine kinases and GPCRs) (45-47) and shallow anterior-posterior gradient of Gβ subunits (48, 49) have failed to account for the observed signaling gradient. Because GIV localizes to the plasma membrane at the leading edge of migrating cells (1, 3, 4, 8), we propose that tyrosine phosphorylated GIV could contribute to the generation and/or maintenance of the steep PI3K signaling gradient observed at the leading edge of migrating cells.

The Phosphotyrosines of GIV Directly Bind p85α

We also provide the structural basis for GIV's association with the p85α regulatory domain of PI3K. Upon phosphorylation GIV directly interacts with p85α through its two C-terminally located phosphotyrosines, Tyr^{1764} and Tyr^{1798}. Both tyrosines are substrates for EGFR and Src and tyrosine-phosphorylated GIV interacted with both N- and C-terminal SH2 domains of p85α. The ability of the phosphotyrosines of GIV to bind both SH2 domains of p85α is in accordance with the structural similarity between the N- and C-terminal SH2 domains of p85α (21), and the ability of both domains to recognize and bind similar phosphotyrosine sequences (21). The sequences flanking these two tyrosine residues in GIV differ from the canonical, p85α-binding YXXMX consensus (50) and instead resemble other non-canonical p85α-binding sequences. The pY^{1798}ATLP peptide shares homology with the pY^{343}LVL peptide from EPO receptor (50), the pY^{1764}FISS peptide shares homology with the pYEPTG peptide from Syk (51) or the pYVNTT peptide in Tie2 (33) which bind the C-terminal SH2 domain of p85α with high affinity and specificity. Thus, the pY^{1764}FISS motif of GIV and its counterparts in Syk and Tie2 are a non-canonical class of peptides with a pYXX[ST] consensus.

We noted that the spacing of GIV's phosphotyrosines and the distance between the two SH2 domains of p85α (28) is compatible with the possibility that the tandem C-terminal phosphotyrosines of GIV simultaneously occupy the tandem SH2 domains of p85α. Previous work has established that such double-occupancy of p85α-SH2 domains in-tandem is required for full activation of the catalytic p110 subunit, presumably through one of the two proposed mechanisms—by triggering allosteric conformational changes (53) or by promoting kinase oligomerization (53). Compared to single occupancy, in-tandem double occupancies in the tyrosine-SH2 signaling pathway confers substantially higher affinity and enhanced biological specificity (52, 54). Whether the biological specificity and potency of PI3K activation by the phosphotyrosines of GIV we observe stems from similar in-tandem interactions remain to be investigated. We conclude that binding of tyrosine phosphorylated GIV to the SH2 domains of p85α provides a mechanism by which signals could be transmitted directly from activated tyrosine kinases to PI3K.

GIV Enhances the Formation of Receptor-PI3K Complexes

We found that tyrosine-phosphorylated GIV facilitated recruitment of p85α to activated EGFR and insulin receptor. Wild-type GIV bound ligand-activated receptor tyrosine kinases, was phosphorylated on the C-terminal tyrosine residues which directly bound the p85α-subunit of PI3K. In the case of the GIV mutant lacking the C-terminal tyrosine phosphorylation sites, binding to ligand-activated receptors was intact, but phosphorylation could take place and p85α recruitment to receptor was reduced (perhaps due to a dominant negative effect of this mutant obscuring other sites for adaptor binding). Previous work has established that the SH2 domains of p85α bind with high affinity to autophosphorylation sites on the cytoplasmic tails of certain receptor tyrosine kinases, and in doing so, are primarily responsible for the binding of PI3K to activated growth factor receptors (55). To date, such high-affinity, direct p85α-binding sites have been described only among receptors of the PDGFR family, such as PDGFR, Kit, and CSF-1 (56). Although several receptors (VEGFR, insulin receptor β, EGFR, and IGFR) interact with the SH2 domains of p85α upon autophosphorylation, these interactions are either weaker than that observed between PDGFR and p85α [as in the case of EGFR (56) and IGFR (57)], or are yet to be demonstrated to be direct [as in the case of VEGFR (58) and the insulin receptor (59)]. Although other adaptors - Grb2 and Gab1 in the case of EGFR, and IRS1 in the case of InsR - can indirectly couple p85α to receptor tyrosine kinases, a specific biological role for PI3K activation through these linkers remain to be established (60). We propose that simultaneously binding of GIV to receptors and p85α may stabilize receptor tyrosine kinase-PI3K complexes in cells and may provide a mechanism by which PI3K signals are amplified directly by GIV at the immediate post-receptor level during cell migration.

The GEF and Phosphotyrosine Motifs of GIV Enhance Activation of Distinct Subclasses of PI3Ks

Our findings identify tyrosine phosphorylation of the C-terminus of GIV as a key underlying event that triggers enhancement of PI3K activation through GIV. We previously demonstrated an obligate requirement also of the GEF motif of GIV for enhancement of PI3K-Akt signaling (7). The GEF motif of GIV is separated from the critical phosphotyrosine motifs by ~80-110 amino acids. Here we provide evidence that these two motifs function independently of each other. In the current work we define the direct link between GIV's phosphotyrosines and p85α, which is a Class 1A PI3K (19). We previously defined the link between activation of Gi by the GEF motif of GIV and activation of PI3K (7): GIV activates G protein, releases ‘free’ Gβγ subunits (7), which in turn bind and activate p110γ(PI3K) (61, 62), a class 1B PI3K, and to some extent p110β, a class 1A PI3K (63). Thus, we propose (**Fig 6D**) that enhancement of cellular PI3K activity by GIV requires simultaneous activation of two parallel pathways: (i) GIV binds p85α regulatory subunits of class 1A PI3K, and (ii) GIV activates Gi and releases free Gβγ, which then binds p110 catalytic subunits of class 1A and 1B PI3Ks (1, 3, 4). Although our results demonstrate that both pathways are required for full activation of the GIV-PI3KAkt axis, the relative contributions of each pathway remain unknown and may vary depending on whether growth factor receptors or GPCRs are stimulated.

We also provide evidence that the ability of GIV to enhance Akt through the GIV-PI3K-Akt axis increases Akt-dependent phosphorylation of GIV at Ser^{1416}, a key phosphorylation event that activates or triggers many biological functions of GIV (1, 3, 4, 39, 40, 42). Although tyrosine phosphorylation of GIV was a prerequisite for efficient phosphorylation of GIV at Ser^{1416} by Akt, presumably through enhancement of Akt activity, phosphorylation at Ser^{1416} did not alter the tyrosine phosphorylation of GIV. These findings suggest a distinct hierarchy in signal transduction: the GIV-PI3K-Akt axis operates upstream at an immediate post-receptor level to amplify incoming PI3K-Akt signals, and possibly receives regulatory feed-back from the downstream Akt-GIV axis wherein Akt phosphorylates and triggers GIV's biological functions (**Fig 6D**). Such a hierarchy or feed-back loop may not be universally operational, because GIV may still be phosphorylated by Akt in certain cell lines, irrespective of whether it plays a major role in enhancement of Akt activity in those cells (40). Our results provide insights into how GIV's function as both an enhancer of Akt activity and as a substrate of Akt might be intertwined.

Tyrosine Phosphorylation of GIV and its Association with p85α May Increase During Cancer Progression

The activation of PI3K-Akt pathway is frequently increased during cancer invasion (38, 64), and progressive enhancement of PI3K-Akt coupled to efficient cell migration is a hallmark of high metastatic potential (38). We previously reported (2, 8, 9) that higher metastatic potential is associated with higher abundance of GIV mRNA and protein in breast and colon carcinomas, and others (3, 4) have demonstrated that GIV is required for tumor cell invasion and VEGF-mediated neoangiogenesis during cancer metastasis. Here we show that tyrosine phosphorylation of GIV and the abundance of GIV-p85α complexes were increased in a breast carcinoma cell during metastatic progression. These changes in GIV's properties among 21T cells coincide with the previously observed (69) increases in the extent of Akt phosphorylation, efficacy of migration, and invasiveness in mouse models of cancer metastasis. It is possible that the observed increases in tyrosine phosphorylation of GIV and the abundance of GIV-p85α complexes in breast carcinoma cells lead to activation of the GIV-PI3KAkt axis during cancer metastasis. Finally, this axis is assembled exclusively in cancer cells and tumors with high invasiveness because GIV's C-terminally located phosphotyrosines are excluded in an alternative spliced, truncated GIVΔCT variant we reported (10) to exist in poorly invasive breast and colon cancer cell lines and non-invasive colorectal carcinomas. Our findings suggest that the GIV-PI3KAkt axis may substantially contribute towards increased activation of the PI3K-Akt pathway observed during cancer invasion. Whether abolishing phosphorylation of the C-terminal tyrosine residues of GIV or disruption of the GIV-p85α interface are feasible therapeutic strategies to halt cancer progression or whether detection of phosphotyrosine-GIV can be a prognosticator of survival remains to be investigated.

In conclusion, we have demonstrated that GIV is a central hub for PI3K activation within tyrosine-based signaling networks, upon which multiple receptors converge in order to enhance Akt activity. The mechanistic and structural insights gained herein not only characterize a new pharmacological target for the regulation of PI3K activity, but also define

the previously elusive links between receptors, GIV, and its role in enhancing Akt activation during cell migration.

MATERIALS AND METHODS

Reagents and Antibodies

Unless otherwise indicated all reagents were of analytical grade and obtained from Sigma-Aldrich (St. Louis, MO). Cell culture media were purchased from Invitrogen (Carlsbad, CA). Epidermal growth factor (EGF) and Insulin were obtained from Invitrogen and Novagen, respectively. Recombinant EGFR, VEGFR and PDGFRβ were purchased from Cell Signaling. PP2 was obtained from Calbiochem. Silencer Negative Control scrambled (Scr) siRNA and Gαi3 siRNA (8) were purchased from Ambion and Santa Cruz, respectively, whereas GIV siRNA (2, 7, 8) was custom ordered from Dharmacon. Antibodies against GIV that were used in this work include rabbit serum and affinity purified anti-GIV coiled-coil IgG (GIV-ccAb; for immunoblotting only) raised against the coiled coil domain of GIV (2, 7, 8), and affinity purified anti-girdin C-terminus (GIV-CTAb; for immunoprecipitation) raised against the last 19 amino acids of the C-terminus of GIV (IBL America, Minnesota and Santa Cruz Biotechnology). Total EGFR was visualized by immunofluorescence with monoclonal antibody #225 raised against the ectodomain (gift from Gordon Gill, UCSD (65)) or anti-EGFR polyclonal antibody (Santa Cruz). Mouse monoclonal antibodies against phosphotyrosine (pTyr, BD Bioscsiences, Cat# 610000), FLAG (Sigma, for immunoprecipitation), polyhistidine (Sigma), GFP (Living Colors, Invitrogen), HA (Covance), and tubulin (Sigma) were purchased from commercial sources. Rabbit polyclonal antibodies against FLAG (Invitrogen; for immunoblotting), p85α (Millipore Inc.), Gαi3 (M-14; Santa Cruz Biotechnology), phospho-Akt S473 (Cell Signaling), pan-Gβ (Santa Cruz Biotechnology), and phospho-ERK 1/2 (Cell Signaling) were obtained commercially. Anti-mouse and anti-rabbit Alexa-594- and Alexa-488-coupled goat secondary antibodies for immunofluorescence were purchased from Invitrogen. Goat anti-rabbit and goat anti-mouse Alexa Fluor 680 or IRDye 800 F(ab')2 for immunoblotting were from Li-Cor Biosciences (Lincoln, NE). Control mouse and rabbit IgGs for immunoprecipitations were purchased from BioRad (Hercules, CA) and Sigma (St. Louis, MO), respectively.

Plasmid Constructs and Mutagenesis

Cloning of Gαi3 and GIV into pGEX-4T-1 or pET28b was described previously (7). GST-EGFR-T (aa 1046 to 1210) was cloned into pGEX-4T-1 based on the reported sequence (NM_005228) as described previously (7). For mammalian expression, C-terminal FLAG-tagged GIV was generated by cloning GIV into p3XFLAG-CMV-14 between Not I and Bam H1. RNAi-resistant GIV was generated by silent mutations as described previously (7). FLAG-GIV and His-GIV-CT phospho-mutants (Y1764F, Y1798F and Y1764,1798F) were generated by site-directed mutagenesis using QuickChange kit (Stratagene, San Diego, CA) as per manufacturer's protocols. GSTSrc (aa 1-257, accession # NM_001025395) was cloned into pGEX-4T-1 between EcoRI and BamH1. C-terminal HA-tagged c-Src for mammalian expression was generated by cloning the entire coding sequence into pcDNA 3.1 between XhoI and EcoRI. The following plasmids and constructs were generous gifts

from other investigators: un-tagged-EGFR (66) and GST-TrkA-CT (aa 448–552) construct encoding the 75-amino acid, juxtamembrane region of rat TrkA from Marilyn G. Farquhar (UCSD) (67); GST-p85 N and C-SH2 constructs from Raju Rajala (University of Okalahoma Health Sciences Center, OK) (59); GST-Grb2 and Gab1 from Marina Holgado-Madruga (Stanford, CA) (68); GFP-Akt-PH from Roger Tsien (University of California, San Diego); GFP-Btk-PH from Seth J. Field (University of California, San Diego); GST-PLCγ1 N and C-SH2 from Tony Pawson (Samuel Lunenfeld Research Institute, Canada) (55); p85α-HA from Hamid Band (UNMC-Eppley Cancer Center, Omaha, NE) (69). All constructs were checked by DNA sequencing.

Protein expression and purification

GST, GST-Gαi3, GST-EGFR-T (aa 1046-1210), GST-TrkA-CT (aa 448-552), the various GST-SH2 adaptors (p85-NSH2, p85-CSH2, Src-SH2, Gab1, Grb2), His-Gαi3, His-GIV-CT WT (aa 1660-1870) and phosphomutants (Y1764F, Y1798F and Y1764,1798F) constructs were expressed and purified from E. coli strain BL21(DE3) (Invitrogen) as described previously (7, 70). Briefly, cultures of transformed bacteria were induced overnight at 25°C with 1 mM isopropyl β-D-1-thiogalactopyranoside (IPTG), bacterial pellet from 1 L of culture was re-suspended in 10 ml GST-lysis buffer [25 mM Tris-HCl, pH 7.5, 20 mM NaCl, 1 mM EDTA, 20% (v:v) glycerol, 1% (v:v) Triton X-100, 2X protease inhibitor cocktail (Complete EDTA-free, Roche Diagnostics)] or His-lysis buffer [50 mM NaH_2PO_4 pH 7.4, 300 mM NaCl, 10 mM imidazole, 1% (v:v) Triton X-100, 2X protease inhibitor cocktail (Complete EDTA-free, Roche Diagnostics)] for GST or His-fused proteins, respectively. After sonication (4 x 20s, 1 min between cycles), lysates were centrifuged at 12,000g at 4°C for 20 min. Solubilized proteins were affinity purified on glutathione-Sepharose 4B beads (GE Healthcare) or HisPur Cobalt Resin (Pierce). Proteins were eluted, dialyzed overnight against PBS and stored at -80 °C. His-Gαi3 was buffer exchanged into G protein storage buffer (20 mM Tris-HCl, pH 7.4, 200 mM NaCl, 1 mM $MgCl_2$, 1 mM DTT, 10 μM GDP, 5% (v:v) glycerol) prior to storage at -80 °C.

In vitro and cellular phosphorylation assays

In vitro kinase assays were performed using bacterially expressed His (6 x His, hexahistidine) tagged GIV-CT (His-GIV-CT, aa 1660-1870) proteins (~10-15 μg per reaction), and recombinant kinases which were obtained commercially (EGFR, Millipore Inc. and Cell Signaling; c-Src, VEGFR2 and PDGFRβ, Cell Signaling) or expressed in bacteria (GST-TrkA kinase domain). Reactions were started by adding 200-1000 μM ATP and carried out at 25°C for 60 min in tyrosine kinase buffer [60 mM HEPES pH 7.5, 5 mM MgCl2, 5 mM MnCl2, 3 μM Na_3OV_4]. Reactions were stopped by addition of Laemmli sample buffer and boiling at 100°C. For cellular phosphorylation assays on endogenous GIV (**Fig 1B** and **S1**), HeLa cells were serum starved for 12-16 hours, pre-incubated with 100 μM sodium orthovanadate and where indicated, the Src-inhibitor PP2 (250 nM) for 1 hour prior to EGF (50 nM) , insulin (100 nM) or LPA (20 μM) stimulation. Reactions were stopped using PBS chilled at 4°C, supplemented with 200 μM sodium orthovanadate, and immediately scraped and lysed for immunoprecipitation. For cellular phosphorylation assays using overexpressed GIV, FLAG-tagged GIV was coexpressed with untagged EGFR (**Fig 1E**) or HA-tagged Src (**Fig 1F**), and at 32 hours after transfection cells were processed as

described above. Tyrosine phosphorylation was analyzed by immunoblotting using anti-pTyr mAb (BD Biosciences).

Phosphopeptide enrichment and LC-MS/MS analysis

In vitro-phosphorylated His-GIV-CT protein was resuspended, reduced with TCEP and carboxymethylated with iodoacetamide prior to digestion with trypsin. Samples were then processed as described previously (71), and the phosphopeptides were enriched using TiO2 (72) before their separation and analysis using nano-flow high pressure liquid chromatography (HPLC) coupled with tandem mass spectroscopy (LC-MS/MS) using a QSTAR-Elite hybrid mass spectrometer (ABSciex®) (73). The collected data was searched using Protein Pilot 2.0 (ABSciex®) and MASCOT (Matrix Science®) for sequence identifications.

Cell Culture, Transfection and Lysis

Unless mentioned otherwise, cell lines used in this work were cultured according to ATCC guidelines. Transfection was carried out using Genejuice (Novagen) for DNA plasmids or Oligofectamine (Invitrogen) for siRNA oligos following the manufacturers' protocols, and stable cell lines were selected as mentioned previously (2, 7) using the neomycin analogue G418 (Cellgro). HeLa cell lines stably expressing GIV-WT (HeLa-GIV-WT), GIV-F1685A mutant (HeLa-GIV-FA) and GIV-Y1764,1798F mutant (HeLa-GIV-YF) were generated and maintained in the presence of G418 (500 μg/ml)as previously described. Clones were chosen for each construct that had relatively low abundance of exogenous expressed GIV (~2 times the abundance of endogenous GIV). For each construct, similar results were obtained from two separate clones. The 21T breast cell lines (16N, NT and MT2) were obtained from Arthur B. Pardee (Dana-Farber Cancer Institute and Harvard Medical School, Boston, MA) and maintained as described previously (37, 38).

Lysates for immunoprecipitation or pull-down assays were prepared by resuspending cells in lysis buffer [20 mM HEPES, pH 7.2, 5 mM Mg-acetate, 125 mM K-acetate, 0.4% Triton X-100, 1 mM DTT, supplemented with sodium orthovanadate (500 μM), phosphatase (Sigma) and protease (Roche) inhibitor cocktails], after which they were passed through a 30G needle at 4°C, and cleared (10-14,000g for 10 min) before use in subsequent experiments.

Steady-state GTPase assay

These assays were done as described previously (2, 7, 8). Briefly, 100 nM of His-Gαi3 was preincubated with different concentrations of sham-treated or in vitro EGFR-phosphorylated His-GIV-CT (aa 1660-1870) for 15 min at 30°C in assay buffer [20 mM Na-HEPES, pH 8, 100 mM NaCl, 1 mM EDTA, 2 mM $MgCl_2$, 1 mM DTT, 0.05% (w:v) C12E10]. GTPase reactions were initiated at 30°C by adding an equal volume of assay buffer containing 1 μM [γ-^{32}P]GTP (~50 c.p.m/ fmol). Duplicate aliquots (50 μl) were removed at 10 min and reactions stopped with 950 μl ice-cold 5% (w/v) activated charcoal in 20 mM H_3PO_4, pH 3. Samples were then centrifuged for 10 min at 10,000 × g, and 500 μl of the resultant supernatant were scintillation counted to quantify released [^{32}P]P_i. To determine the specific Pi produced, the background [^{32}P]P_i detected at 10 min in the absence of G protein was

subtracted from each reaction. The results were expressed either as absolute values of Pi produced.

Immunofluorescence

Cells were fixed at room temperature with 3% paraformaldehyde for 20-25 min, permeabilized (0.2% Triton X-100) for 45 min and incubated for 1 hour each with primary and then secondary antibodies as described previously (8). Antibody dilutions were as follows: mAb GFP, 1:500; secondary goat anti-rabbit (594) and goat anti-mouse (488) Alexa-conjugated antibodies, 1:500, and DAPI, 1:2000 (Molecular Probes). Samples were examined with a Zeiss Axiophot microscope (Carl Zeiss Inc., Thornwood, NY) using a 63 x aperture (Zeiss Plan Neofluar, 1.30 NA), and images were collected with the ORCA-ER camera Hamamatsu, Bridgewater, NJ), and Volocity Software. All individual images were processed using Image J software (NIH) and assembled for presentation using Photoshop and Illustrator software (both Adobe).

GST-pulldown and Immunoprecipitation Assays

These assays were carried out as previously described (24) with minor modifications. Purified GST-fused proteins (15-35 μg) or GST alone (30-45 μg) were immobilized on glutathione *S*-sepharose beads (GE healthcare) and incubated for 4 hours at 4°C in binding buffer (50 mM Tris-HCl, pH 7.4, 100 mM NaCl, 0.4% (v:v) NP-40, 10 mM $MgCl_2$, 5 mM EDTA, 2 mM DTT, and 2 mM Sodium Orthovanadate) containing sham-treated or in vitro phosphorylated His-GIV CT (aa 1660-1870). After a 4 hour incubation at 4°C, the beads were washed (4.3 mM Na_2HPO_4, 1.4 mM KH_2PO_4, pH 7.4, 137 mM NaCl, 2.7 mM KCl, 0.1% (v:v) Tween 20, 10 mM $MgCl_2$, 5 mM EDTA, 2 mM DTT, and 30 and 2 mM Sodium Orthovanadate), and bound proteins eluted in sample buffer for SDS-PAGE. When GST-Gαi3 was used in these assays, both binding and wash buffers were supplemented with 30 μM GDP. Where indicated, His-GIV CT was phosphorylated in vitro using recombinant EGFR (Invitrogen) prior to its use in pulldown assays.

For immunoprecipitations, cell lysates (~1-2 mg protein) were incubated for 4 hours at 4°C with either 2 μg anti-FLAG mAb for immunoprecipitation of GIV-FLAG, anti-GIV-CT (Girdin-T13 Ab, Santa Cruz Biotechnology) for endogenous GIV, anti-HA mAb (Covance) for immunoprecipitation of HA-tagged insulin receptor, anti-EGFR #225 mAb (65) for immunoprecipitation of endogenous EGFR, and their respective pre-immune control IgGs where indicated. Protein A (for GIV-CT Ab) or G (for all other mAbs) agarose beads (GE healthcare) were added and incubated at 4°C for an additional 60 min. Beads were washed then either resuspended and boiled in SDS sample buffer. Buffers were supplemented with 1 mM sodium orthovanadate for all steps of the assay.

Molecular Modeling of the GIV-p85 interface

The initial coordinates for C-terminal and N-terminal SH2-domains of p85α were taken from their crystal structures bound to the PDGFRβ peptide, pY^{751}VPML (24) and c-Kit phosphotyrosyl peptide (25), respectively. Structural models of GIV's phosphotyrosine peptides, EDTpY^{1764}FISS and SNPpY^{1798}ATLP were initially generated with ideal covalent geometry. Backbone atoms of the peptides and heavy atoms of the phosphorylated

tyrosine side-chain were tethered to their respective counterparts in the PDGFRβ or cKit peptide templates using soft harmonic restraints and subjected to several rounds of Monte Carlo optimization with decreasing tether weight. During the optimization, the backbone conformation of the SH2 domain was held constant and torsional angles controlling the side-chains of both molecules and the backbone of the GIV phosphotyrosine peptide were fully sampled.

PI3K Assay

The method we used here is largely adapted from published protocols (27-31) with minor modifications. Cos7 cells plated at 80-85% confluency were cotransfected with p85α-HA and either wild-type (WT) or YF mutant of GIV-FLAG. Vector-transfected Cos7 cells were used as controls. 48 hours after transfection, cells were lysed in the lysis buffer [20 mM HEPES, pH 7.2, 5 mM Mg-acetate, 125 mM K-acetate, 0.4% Triton X-100, 1 mM DTT, supplemented with sodium orthovanadate (500 μM), phosphatase (Sigma) and protease (Roche) inhibitor cocktails], and equal aliquots of lysates were treated with 2 μg of anti-HA mAb (Covance) for 3 hours and protein G agarose beads for 45 min to immunoprecipitate p85α (PI3K). The bead-bound immune complexes were subsequently washed two times using each of the 4 different wash buffers, in the following order: (i) phosphate-buffered saline, 100 mM sodium orthovanadate, 1% Triton X-100; (ii) 100 mM Tris/HCl, pH 7.4, 5 mM LiCl and 0.1 mM sodium orthovanadate, (iii) TNE buffer [10 mM Tris/HCl, pH 7.4, 150 mM NaCl, 5 mM EDTA and 0.1 mM sodium orthovanadate] and, (iv) 20 mM HEPES, pH 7.5, 50 mM NaCl, 5 mM EDTA, 30 mM sodium pyrophosphate, 200 mM sodium orthovanadate, protease inhibitors, 0.03% Triton X-100. The washed beads were resuspended in 70 μl buffer and the reaction started by the simultaneous addition of 10 μl 10x ATP stock solution (65 mM HEPES, pH 7.0, 100 mM $MgCl_2$, 500 μM ATP and 10 μCi [γ-^{32}P] ATP (specific activity > 5,000 Ci/mmol) and 20 μl freshly reconstituted 1mg/ml L-α-phosphatidylinositol (from bovine liver, Sigma) in 20 mM HEPES pH 7.0, 1 mM EDTA. After incubation for 10 min at room temperature the reactions were terminated by adding 25 μl 5M HCl and vortexing. Lipids were extracted by addition of 160 μl 1:1 mix of methanol:chloroform and vortexing. Organic and water soluble phases were separated by centrifugation for 2 min at room temperature in a microfuge. Equal aliquots of the lower organic phase were loaded immediately onto TLC plates (previously heat activated at 100 °C for 45 min) which were run in a tank equilibrated with the a solvent mixture of chloroform:methanol:water:ammonium hydroxide (60:47:11.3:2) and subsequently analyzed by autoradiography.

Statistical Analysis

Each experiment presented in the figures is representative of at least three independent experiments. Statistical significance (*p* value) between various conditions was assessed with the one-way ANOVA (Bonferroni posthoc test) . All graphical data presented was prepared using GraphPad Software, Inc., San Diego, CA.

Supplementary Material

Refer to Web version on PubMed Central for supplementary material.

Acknowledgments

We thank Marilyn G. Farquhar and Gordon N. Gill (UCSD) for scientific advice and thoughtful comments during preparation of this manuscript; Jasmine Wong and Andrew Ong (Undergraduate students, UCSD) for assistance with protein expression and purification, and members of the UCSD Mass Spectrometry Core Facility, of which Majid Ghassemian is the director.

Funding: Supported by Burroughs Wellcome Fund, Doris Duke Charitable Foundation and Research Scholar Award (American Gastroenterology Association FDN) to P.G. MG-M was supported by Susan G. Komen Postdoctoral fellowship KG080079; M.G. is supported by SRP Super Fund Research Program; R.A. is supported by R01 GM 071872; Yash Mittal is supported by Sarah Rogers Fellowship (UCSD) and Jason Ear was supported by the Mc Nair Scholarship Program.

REFERENCES

1. Enomoto A, Murakami H, Asai N, Morone N, Watanabe T, Kawai K, Murakumo Y, Usukura J, Kaibuchi K, Takahashi M. Akt/PKB regulates actin organization and cell motility via Girdin/APE. Developmental cell. 2005; 9:389–402. [PubMed: 16139227]
2. Ghosh P, Beas AO, Bornheimer SJ, Garcia-Marcos M, Forry EP, Johannson C, Ear J, Jung BH, Cabrera B, Carethers JM, Farquhar MG. A Gi-GIV Molecular Complex Binds Epidermal Growth Factor Receptor and Determines whether Cells Migrate or Proliferate. Molecular biology of the cell. 2010
3. Jiang P, Enomoto A, Jijiwa M, Kato T, Hasegawa T, Ishida M, Sato T, Asai N, Murakumo Y, Takahashi M. An actin-binding protein Girdin regulates the motility of breast cancer cells. Cancer research. 2008; 68:1310–1318. [PubMed: 18316593]
4. Kitamura T, Asai N, Enomoto A, Maeda K, Kato T, Ishida M, Jiang P, Watanabe T, Usukura J, Kondo T, Costantini F, Murohara T, Takahashi M. Regulation of VEGF-mediated angiogenesis by the Akt/PKB substrate Girdin. Nature cell biology. 2008; 10:329–337.
5. Anai M, Shojima N, Katagiri H, Ogihara T, Sakoda H, Onishi Y, Ono H, Fujishiro M, Fukushima Y, Horike N, Viana A, Kikuchi M, Noguchi N, Takahashi S, Takata K, Oka Y, Uchijima Y, Kurihara H, Asano T. A novel protein kinase B (PKB)/AKT-binding protein enhances PKB kinase activity and regulates DNA synthesis. J Biol Chem. 2005; 280:18525–18535. [PubMed: 15753085]
6. Garcia-Marcos M, Ear J, Farquhar MG, Ghosh P. A GDI (AGS3) and a GEF (GIV) regulate autophagy by balancing G protein activity and growth factor signals. Molecular biology of the cell. 2011; 22:673–686. [PubMed: 21209316]
7. Garcia-Marcos M, Ghosh P, Farquhar MG. GIV is a nonreceptor GEF for G alpha i with a unique motif that regulates Akt signaling. Proceedings of the National Academy of Sciences of the United States of America. 2009; 106:3178–3183. [PubMed: 19211784]
8. Ghosh P, Garcia-Marcos M, Bornheimer SJ, Farquhar MG. Activation of Galphai3 triggers cell migration via regulation of GIV. The Journal of cell biology. 2008; 182:381–393. [PubMed: 18663145]
9. Garcia-Marcos M, Jung BH, Ear J, Cabrera B, Carethers JM, Ghosh P. Expression of GIV/Girdin, a metastasis-related protein, predicts patient survival in colon cancer. Faseb J. 2011; 25:590–599. [PubMed: 20974669]
10. Rush J, Moritz A, Lee KA, Guo A, Goss VL, Spek EJ, Zhang H, Zha XM, Polakiewicz RD, Comb MJ. Immunoaffinity profiling of tyrosine phosphorylation in cancer cells. Nature biotechnology. 2005; 23:94–101.
11. Moritz A, Li Y, Guo A, Villen J, Wang Y, MacNeill J, Kornhauser J, Sprott K, Zhou J, Possemato A, Ren JM, Hornbeck P, Cantley LC, Gygi SP, Rush J, Comb MJ. Akt-RSK-S6 kinase signaling networks activated by oncogenic receptor tyrosine kinases. Science signaling. 3:ra64. [PubMed: 20736484]
12. Guo A, Villen J, Kornhauser J, Lee KA, Stokes MP, Rikova K, Possemato A, Nardone J, Innocenti G, Wetzel R, Wang Y, MacNeill J, Mitchell J, Gygi SP, Rush J, Polakiewicz RD, Comb MJ. Signaling networks assembled by oncogenic EGFR and c-Met. Proceedings of the National Academy of Sciences of the United States of America. 2008; 105:692–697. [PubMed: 18180459]

13. Jorgensen C, Sherman A, Chen GI, Pasculescu A, Poliakov A, Hsiung M, Larsen B, Wilkinson DG, Linding R, Pawson T. Cell-specific information processing in segregating populations of Eph receptor ephrin-expressing cells. Science (New York, N.Y. 2009; 326:1502–1509.
14. St-Germain JR, Taylor P, Tong J, Jin LL, Nikolic A, Stewart II, Ewing RM, Dharsee M, Li Z, Trudel S, Moran MF. Multiple myeloma phosphotyrosine proteomic profile associated with FGFR3 expression, ligand activation, and drug inhibition. Proceedings of the National Academy of Sciences of the United States of America. 2009; 106:20127–20132. [PubMed: 19901323]
15. Osherov N, Levitzki A. Epidermal-growth-factor-dependent activation of the src-family kinases. European journal of biochemistry / FEBS. 1994; 225:1047–1053. [PubMed: 7525285]
16. Hanke JH, Gardner JP, Dow RL, Changelian PS, Brissette WH, Weringer EJ, Pollok BA, Connelly PA. Discovery of a novel, potent, and Src family-selective tyrosine kinase inhibitor. Study of Lck- and FynT-dependent T cell activation. The Journal of biological chemistry. 1996; 271:695–701. [PubMed: 8557675]
17. Andreev J, Galisteo ML, Kranenburg O, Logan SK, Chiu ES, Okigaki M, Cary LA, Moolenaar WH, Schlessinger J. Src and Pyk2 mediate G-protein-coupled receptor activation of epidermal growth factor receptor (EGFR) but are not required for coupling to the mitogen-activated protein (MAP) kinase signaling cascade. The Journal of biological chemistry. 2001; 276:20130–20135. [PubMed: 11274221]
18. Enomoto A, Ping J, Takahashi M. Girdin, a novel actin-binding protein, and its family of proteins possess versatile functions in the Akt and Wnt signaling pathways. Annals of the New York Academy of Sciences. 2006; 1086:169–184. [PubMed: 17185515]
19. Cantley LC. The phosphoinositide 3-kinase pathway. Science (New York, N.Y. 2002; 296:1655–1657.
20. Piccione E, Case RD, Domchek SM, Hu P, Chaudhuri M, Backer JM, Schlessinger J, Shoelson SE. Phosphatidylinositol 3-kinase p85 SH2 domain specificity defined by direct phosphopeptide/SH2 domain binding. Biochemistry. 1993; 32:3197–3202. [PubMed: 8384875]
21. Songyang Z, Shoelson SE, Chaudhuri M, Gish G, Pawson T, Haser WG, King F, Roberts T, Ratnofsky S, Lechleider RJ, Neel BG, Birge RB, Fajardo JE, Chou MM, Hanafusa H, Schaffhausen B, Cantley LC. SH2 domains recognize specific phosphopeptide sequences. Cell. 1993; 72:767–778. [PubMed: 7680959]
22. Abagyan R, Totrov M. Biased probability Monte Carlo conformational searches and electrostatic calculations for peptides and proteins. J Mol Biol. 1994; 235:983–1002. [PubMed: 8289329]
23. Abagyan R, Totrov M, Kuznetsov DA. ICM: A New Method for Protein Modeling and Design: Applications to Docking and Structure Prediction from the Distorted Native Conformation. J Comp Chem. 1994; 15:488–506.
24. Pauptit RA, Dennis CA, Derbyshire DJ, Breeze AL, Weston SA, Rowsell S, Murshudov GN. NMR trial models: experiences with the colicin immunity protein Im7 and the p85[alpha] C-terminal SH2-peptide complex. Acta Crystallographica Section D. 2001; 57:1397–1404.
25. Nolte RT, Eck MJ, Schlessinger J, Shoelson SE, Harrison SC. Crystal structure of the PI 3-kinase p85 amino-terminal SH2 domain and its phosphopeptide complexes. Nature structural biology. 1996; 3:364–374.
26. Holt KH, Olson L, Moye-Rowley WS, Pessin JE. Phosphatidylinositol 3-kinase activation is mediated by high-affinity interactions between distinct domains within the p110 and p85 subunits. Molecular and cellular biology. 1994; 14:42–49. [PubMed: 8264609]
27. Cuevas B, Lu Y, Watt S, Kumar R, Zhang J, Siminovitch KA, Mills GB. SHP-1 regulates Lck-induced phosphatidylinositol 3-kinase phosphorylation and activity. J Biol Chem. 1999; 274:27583–27589. [PubMed: 10488096]
28. Whitman M, Downes CP, Keeler M, Keller T, Cantley L. Type I phosphatidylinositol kinase makes a novel inositol phospholipid, phosphatidylinositol-3-phosphate. Nature. 1988; 332:644–646. [PubMed: 2833705]
29. Fry MJ, Gebhardt A, Parker PJ, Foulkes JG. Phosphatidylinositol turnover and transformation of cells by Abelson murine leukaemia virus. The EMBO journal. 1985; 4:3173–3178. [PubMed: 3004937]

30. Wang P, Kumar P, Wang C, Defea KA. Differential regulation of class IA phosphoinositide 3-kinase catalytic subunits p110 alpha and beta by protease-activated receptor 2 and beta-arrestins. The Biochemical journal. 2007; 408:221–230. [PubMed: 17680774]
31. Zhang Z, Yang XY, Soltoff SP, Cohen DM. PI3K signaling in the murine kidney inner medullary cell response to urea. American journal of physiology. 2000; 278:F155–164. [PubMed: 10644667]
32. Kavran JM, Klein DE, Lee A, Falasca M, Isakoff SJ, Skolnik EY, Lemmon MA. Specificity and promiscuity in phosphoinositide binding by pleckstrin homology domains. The Journal of biological chemistry. 1998; 273:30497–30508. [PubMed: 9804818]
33. Kontos CD, Stauffer TP, Yang WP, York JD, Huang L, Blanar MA, Meyer T, Peters KG. Tyrosine 1101 of Tie2 is the major site of association of p85 and is required for activation of phosphatidylinositol 3-kinase and Akt. Mol Cell Biol. 1998; 18:4131–4140. [PubMed: 9632797]
34. Servant G, Weiner OD, Herzmark P, Balla T, Sedat JW, Bourne HR. Polarization of chemoattractant receptor signaling during neutrophil chemotaxis. Science (New York, N.Y. 2000; 287:1037–1040.
35. Watton SJ, Downward J. Akt/PKB localisation and 3' phosphoinositide generation at sites of epithelial cell-matrix and cell-cell interaction. Curr Biol. 1999; 9:433–436. [PubMed: 10226029]
36. Varnai P, Rother KI, Balla T. Phosphatidylinositol 3-kinase-dependent membrane association of the Bruton's tyrosine kinase pleckstrin homology domain visualized in single living cells. The Journal of biological chemistry. 1999; 274:10983–10989. [PubMed: 10196179]
37. Band V, Zajchowski D, Swisshelm K, Trask D, Kulesa V, Cohen C, Connolly J, Sager R. Tumor progression in four mammary epithelial cell lines derived from the same patient. Cancer research. 1990; 50:7351–7357. [PubMed: 1977518]
38. Qiao M, Iglehart JD, Pardee AB. Metastatic potential of 21T human breast cancer cells depends on Akt/protein kinase B activation. Cancer research. 2007; 67:5293–5299. [PubMed: 17545609]
39. Enomoto A, Asai N, Namba T, Wang Y, Kato T, Tanaka M, Tatsumi H, Taya S, Tsuboi D, Kuroda K, Kaneko N, Sawamoto K, Miyamoto R, Jijiwa M, Murakumo Y, Sokabe M, Seki T, Kaibuchi K, Takahashi M. Roles of disrupted-in-schizophrenia 1-interacting protein girdin in postnatal development of the dentate gyrus. Neuron. 2009; 63:774–787. [PubMed: 19778507]
40. Miyake H, Maeda K, Asai N, Shibata R, Ichimiya H, Isotani-Sakakibara M, Yamamura Y, Kato K, Enomoto A, Takahashi M, Murohara T. The actin-binding protein Girdin and its Akt-mediated phosphorylation regulate neointima formation after vascular injury. Circulation research. 2011; 108:1170–1179. [PubMed: 21415395]
41. Yamaguchi M, Suyari O, Nagai R, Takahashi M. dGirdin a new player of Akt /PKB signaling in Drosophila Melanogaster. Front Biosci. 2010; 15:1164–1171.
42. Wang Y, Kaneko N, Asai N, Enomoto A, Isotani-Sakakibara M, Kato T, Asai M, Murakumo Y, Ota H, Hikita T, Namba T, Kuroda K, Kaibuchi K, Ming GL, Song H, Sawamoto K, Takahashi M. Girdin is an intrinsic regulator of neuroblast chain migration in the rostral migratory stream of the postnatal brain. J Neurosci. 2011; 31:8109–8122. [PubMed: 21632933]
43. Ghosh P, Garcia-Marcos M, Farquhar MG. GIV/Girdin is a rheostat that fine-tunes growth factor signals during tumor progression. Cell adhesion & migration. 2011; 5:237–248. [PubMed: 21546796]
44. Haugh JM, Codazzi F, Teruel M, Meyer T. Spatial sensing in fibroblasts mediated by 3' phosphoinositides. The Journal of cell biology. 2000; 151:1269–1280. [PubMed: 11121441]
45. Servant G, Weiner OD, Neptune ER, Sedat JW, Bourne HR. Dynamics of a chemoattractant receptor in living neutrophils during chemotaxis. Molecular biology of the cell. 1999; 10:1163–1178. [PubMed: 10198064]
46. Xiao Z, Zhang N, Murphy DB, Devreotes PN. Dynamic distribution of chemoattractant receptors in living cells during chemotaxis and persistent stimulation. The Journal of cell biology. 1997; 139:365–374. [PubMed: 9334341]
47. Bailly M, Wyckoff J, Bouzahzah B, Hammerman R, Sylvestre V, Cammer M, Pestell R, Segall JE. Epidermal growth factor receptor distribution during chemotactic responses. Molecular biology of the cell. 2000; 11:3873–3883. [PubMed: 11071913]
48. Janetopoulos C, Jin T, Devreotes P. Receptor-mediated activation of heterotrimeric G-proteins in living cells. Science (New York, N.Y. 2001; 291:2408–2411.

49. Jin T, Zhang N, Long Y, Parent CA, Devreotes PN. Localization of the G protein betagamma complex in living cells during chemotaxis. Science (New York, N.Y. 2000; 287:1034–1036.
50. He TC, Zhuang H, Jiang N, Waterfield MD, Wojchowski DM. Association of the p85 regulatory subunit of phosphatidylinositol 3-kinase with an essential erythropoietin receptor subdomain. Blood. 1993; 82:3530–3538. [PubMed: 7505116]
51. Moon KD, Post CB, Durden DL, Zhou Q, De P, Harrison ML, Geahlen RL. Molecular Basis for a Direct Interaction between the Syk Protein-tyrosine Kinase and Phosphoinositide 3-Kinase. Journal of Biological Chemistry. 2005; 280:1543–1551. [PubMed: 15536084]
52. Rordorf-Nikolic T, Van Horn DJ, Chen D, White MF, Backer JM. Regulation of phosphatidylinositol 3'-kinase by tyrosyl phosphoproteins. Full activation requires occupancy of both SH2 domains in the 85-kDa regulatory subunit. J Biol Chem. 1995; 270:3662–3666. [PubMed: 7876105]
53. Layton MJ, Harpur AG, Panayotou G, Bastiaens PI, Waterfield MD. Binding of a diphosphotyrosine-containing peptide that mimics activated platelet-derived growth factor receptor beta induces oligomerization of phosphatidylinositol 3-kinase. J Biol Chem. 1998; 273:33379–33385. [PubMed: 9837914]
54. Ottinger EA, Botfield MC, Shoelson SE. Tandem SH2 domains confer high specificity in tyrosine kinase signaling. J Biol Chem. 1998; 273:729–735. [PubMed: 9422724]
55. McGlade CJ, Ellis C, Reedijk M, Anderson D, Mbamalu G, Reith AD, Panayotou G, End P, Bernstein A, Kazlauskas A, et al. SH2 domains of the p85 alpha subunit of phosphatidylinositol 3-kinase regulate binding to growth factor receptors. Molecular and cellular biology. 1992; 12:991–997. [PubMed: 1372092]
56. Hu P, Margolis B, Skolnik EY, Lammers R, Ullrich A, Schlessinger J. Interaction of phosphatidylinositol 3-kinase-associated p85 with epidermal growth factor and platelet-derived growth factor receptors. Molecular and cellular biology. 1992; 12:981–990. [PubMed: 1372091]
57. Altschuler D, Yamamoto K, Lapetina EG. Insulin-like growth factor-1-mediated association of p85 phosphatidylinositol 3-kinase with pp 185: requirement of SH2 domains for in vivo interaction. Molecular endocrinology (Baltimore, Md. 1994; 8:1139–1146.
58. Cunningham SA, Waxham MN, Arrate PM, Brock TA. Interaction of the Flt-1 tyrosine kinase receptor with the p85 subunit of phosphatidylinositol 3-kinase. Mapping of a novel site involved in binding. J Biol Chem. 1995; 270:20254–20257. [PubMed: 7657594]
59. Rajala RV, Anderson RE. Interaction of the insulin receptor beta-subunit with phosphatidylinositol 3-kinase in bovine ROS. Invest Ophthalmol Vis Sci. 2001; 42:3110–3117. [PubMed: 11726610]
60. Cully M, You H, Levine AJ, Mak TW. Beyond PTEN mutations: the PI3K pathway as an integrator of multiple inputs during tumorigenesis. Nature reviews. 2006; 6:184–192.
61. Maier U, Babich A, Nurnberg B. Roles of non-catalytic subunits in gbetagamma-induced activation of class I phosphoinositide 3-kinase isoforms beta and gamma. J Biol Chem. 1999; 274:29311–29317. [PubMed: 10506190]
62. Stephens L, Eguinoa A, Corey S, Jackson T, Hawkins PT. Receptor stimulated accumulation of phosphatidylinositol (3,4,5)-trisphosphate by G-protein mediated pathways in human myeloid derived cells. The EMBO journal. 1993; 12:2265–2273. [PubMed: 8389691]
63. Guillermet-Guibert J, Bjorklof K, Salpekar A, Gonella C, Ramadani F, Bilancio A, Meek S, Smith AJ, Okkenhaug K, Vanhaesebroeck B. The p110beta isoform of phosphoinositide 3-kinase signals downstream of G protein-coupled receptors and is functionally redundant with p110gamma. Proceedings of the National Academy of Sciences of the United States of America. 2008; 105:8292–8297. [PubMed: 18544649]
64. Larue L, Bellacosa A. Epithelial-mesenchymal transition in development and cancer: role of phosphatidylinositol 3' kinase/AKT pathways. Oncogene. 2005; 24:7443–7454. [PubMed: 16288291]
65. Gill GN, Kawamoto T, Cochet C, Le A, Sato JD, Masui H, McLeod C, Mendelsohn J. Monoclonal anti-epidermal growth factor receptor antibodies which are inhibitors of epidermal growth factor binding and antagonists of epidermal growth factor binding and antagonists of epidermal growth factor-stimulated tyrosine protein kinase activity. J Biol Chem. 1984; 259:7755–7760. [PubMed: 6330079]

66. Zheng B, Lavoie C, Tang TD, Ma P, Meerloo T, Beas A, Farquhar MG. Regulation of epidermal growth factor receptor degradation by heterotrimeric Galphas protein. Molecular biology of the cell. 2004; 15:5538–5550. [PubMed: 15469987]

67. Lou X, Yano H, Lee F, Chao MV, Farquhar MG. GIPC and GAIP form a complex with TrkA: a putative link between G protein and receptor tyrosine kinase pathways. Molecular biology of the cell. 2001; 12:615–627. [PubMed: 11251075]

68. Fixman ED, Holgado-Madruga M, Nguyen L, Kamikura DM, Fournier TM, Wong AJ, Park M. Efficient cellular transformation by the Met oncoprotein requires a functional Grb2 binding site and correlates with phosphorylation of the Grb2-associated proteins, Cbl and Gab1. J Biol Chem. 1997; 272:20167–20172. [PubMed: 9242692]

69. Fukazawa T, Reedquist KA, Panchamoorthy G, Soltoff S, Trub T, Druker B, Cantley L, Shoelson SE, Band H. T cell activation-dependent association between the p85 subunit of the phosphatidylinositol 3-kinase and Grb2/phospholipase C-gamma 1-binding phosphotyrosyl protein pp36/38. J Biol Chem. 1995; 270:20177–20182. [PubMed: 7544353]

70. Garcia-Marcos M, Ghosh P, Ear J, Farquhar MG. A structural determinant that renders G alpha(i) sensitive to activation by GIV/girdin is required to promote cell migration. J Biol Chem. 2010; 285:12765–12777. [PubMed: 20157114]

71. Guttman M, Betts GN, Barnes H, Ghassemian M, van der Geer P, Komives EA. Interactions of the NPXY microdomains of the low density lipoprotein receptor-related protein 1. Proteomics. 2009; 9:5016–5028. [PubMed: 19771558]

72. Pinkse MW, Uitto PM, Hilhorst MJ, Ooms B, Heck AJ. Selective isolation at the femtomole level of phosphopeptides from proteolytic digests using 2D-NanoLC-ESI-MS/MS and titanium oxide precolumns. Analytical chemistry. 2004; 76:3935–3943. [PubMed: 15253627]

73. McCormack AL, Schieltz DM, Goode B, Yang S, Barnes G, Drubin D, Yates JR 3rd. Direct analysis and identification of proteins in mixtures by LC/MS/MS and database searching at the lowfemtomole level. Analytical chemistry. 1997; 69:767–776. [PubMed: 9043199]

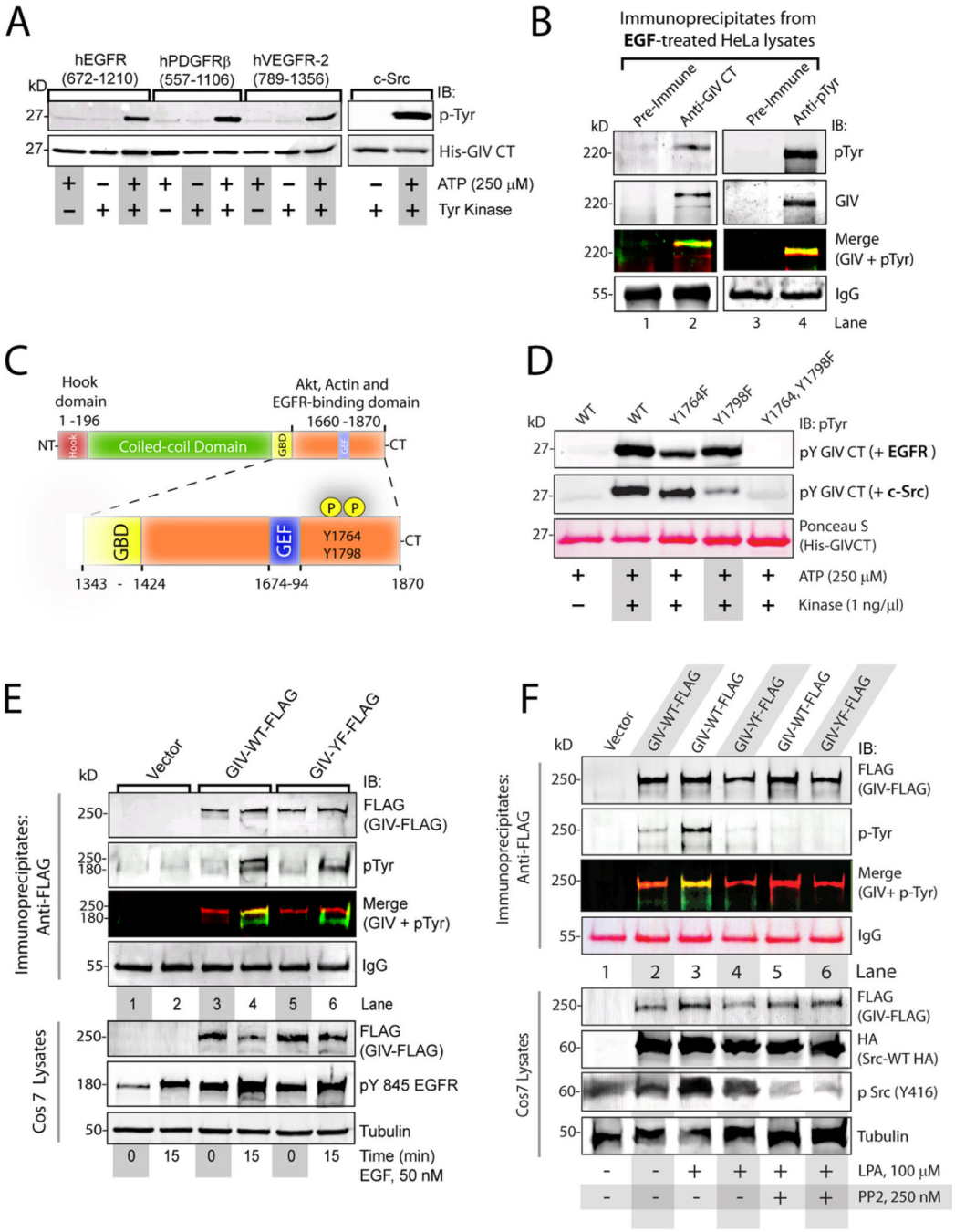

Figure 1. GIV is phosphorylated on Tyr^{1764} and Tyr^{1798} by receptor and non-receptor tyrosine kinases

A. In vitro kinase assays using the indicated recombinant tyrosine kinases were carried out on the His-tagged C-terminus domain of GIV (His-GIV CT) and immunoblotted (IB) for tyrosine phosphorylation. **B.** GIV (lane 2; preimmune IgG, lane 1) and phosphotyrosine proteins (lane 4; preimmune IgG, lane 3) were immunoprecipitated from EGF-treated HeLa cells and analyzed by two-color immunoblotting (IB) for GIV and pTyr. Single channel images for GIV and pTyr are displayed in grayscale and the overlay of GIV-red and pTyr (green) images in the merged panels. **C.** Tyr^{1764} and Tyr^{1798} are located in the C-terminus

within the EGFR, Akt and actin-binding domains (orange) and were the only sites of tyrosine phosphorylation identified by phosphoproteomic analysis (**Fig S3**). **D.** In vitro kinase assays using recombinant EGFR (top panel) and c-Src (middle panel) on wild-type (WT), Y1764F, Y1798F, and Y1764, Y1798F mutants of His-GIV CT (Ponceau S, bottom panel) were analyzed for tyrosine phosphorylation. **E.** Cos7 cells expressing FLAG-tagged wild-type GIV (GIV-WT-FLAG), a tyrosine phosphorylation deficient mutant (GIV-YF-FLAG), or vector alone were serum starved or stimulated with EGF. FLAG immunoprecipitates (top) were analyzed by two-color immunoblotting for GIV and pTyr. **F.** Cos7 cells expressing c-Src-HA and GIV-WT-FLAG, GIV-YF-FLAG, or vector control were serum starved, incubated with or without PP2, and stimulated with LPA. Src was inhibited by PP2 as determined by decreased phosphorylation of Src at Tyr^{416}. FLAG immune complexes (top panels) were analyzed by two-color immunoblotting (IB) for GIV and pTyr. Tyrosine phosphorylation occurred in GIVWT-FLAG expressing cells upon ligand stimulation and in the absence of PP2 (lane 3). GIV-WT-FLAG was tyrosine phosphorylated (Merge) after LPA stimulation (lane 3), but not when Src was inhibited with PP2 (lane 5). GIV-YF is not tyrosine phosphorylated (lanes 4 and 6).

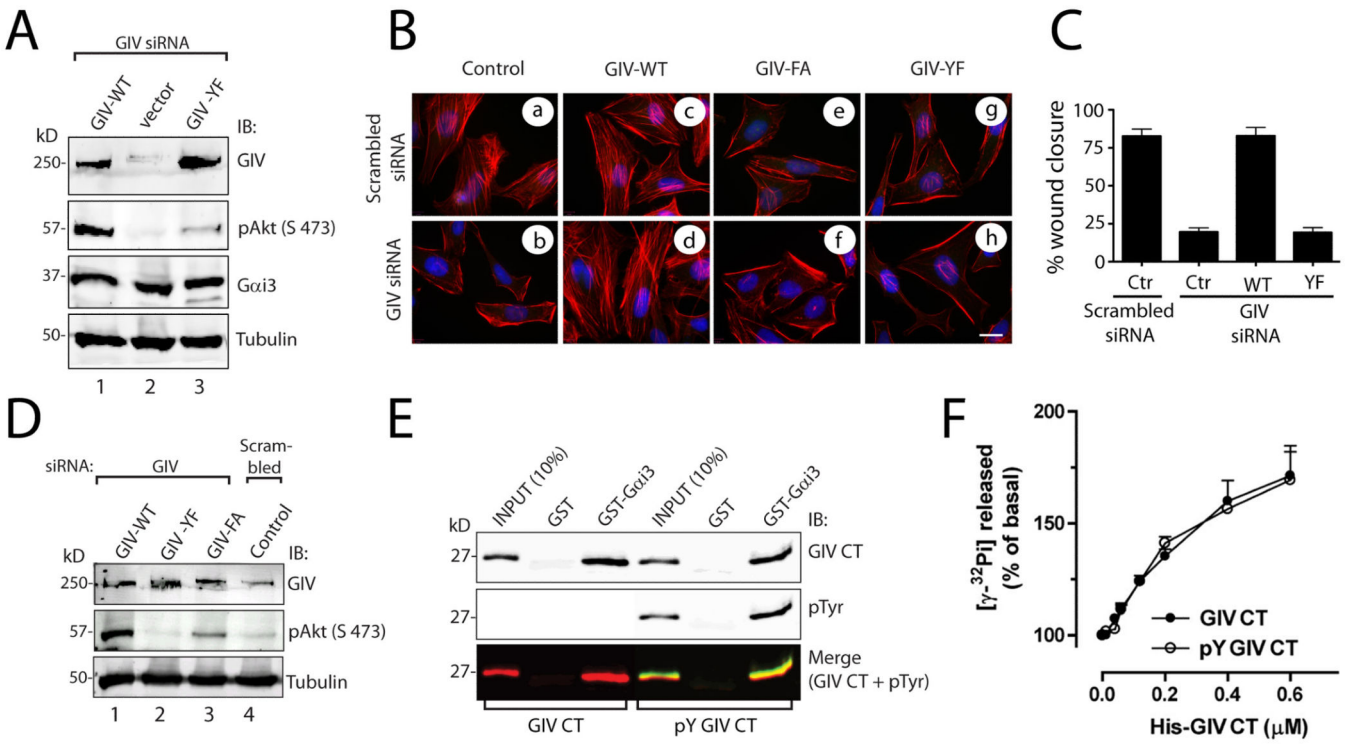

Figure 2. Tyrosine phosphorylation of GIV does not affect its ability to bind or activate Gαi, but is required for phosphorylation of Akt, actin remodeling, and cell migration

A. HeLa cells stably expressing control vector or siRNA resistant GIV-WT-FLAG or GIV-YF-FLAG plasmids were transfected with GIV siRNA. Lysates were immunoblotted for GIV, phospho-Akt (pAkt), Gαi3, and tubulin. Phosphorylation of Akt (pAkt) was significantly reduced in GIV-depleted control cells (lane 2) and GIV-YF cells (lane 3) compared to GIV-WT cells (lane 1). $p < 0.001$ for both sets of comparisons; N = 3 experiments. **B.** HeLa cells stably expressing vector (control), siRNA resistant GIV-WT-FLAG, GIV-FA-FLAG (the GEF-deficient mutant), or GIV-YF-FLAG plasmids were treated with scrambled or GIV siRNA as indicated. Cells were costained with phalliodin-Texas red (F-actin, red) and DAPI (DNA, blue). Depletion of GIV in control cells resulted in loss of stress fibers, which were restored by expression of siRNA resistant GIV-WT-FLAG, but not GIV-FA-FLAG or GIV-YF-FLAG. Bar = 10 μM. **C.** Untransfected HeLa cells (control; Ctr), HeLa-GIV-WT, HeLa-GIV-FA, and HeLa-GIV-YF cells were transfected with scrambled or GIV siRNA. Results are shown as mean ± S.D. of 8-12 randomly chosen fields from n=3 experiments. $p < 0.001$ for either sets of comparisons between Ctr and GIV-depleted cells and between GIV-WT-FLAG and GIV-YF-FLAG cells. **D.** Control HeLa cells and HeLa cells stably expressing siRNA resistant GIV-WT-FLAG, GIV-YF-FLAG, and GIV-FA-FLAG plasmids were transfected with scrambled and GIV siRNA and immunoblotted for GIV, phospho-Akt (pAkt), and tubulin. *p* -values for both comparisons between GIV-WT-FLAG and GIV-FA-FLAG and between GIV-WT-FLAG and GIVYF-FLAG are < 0.001; N = 3 experiments. (**E**) Mock-treated His-GIV-CT and in vitro EGFR-phosphorylated His-GIV-CT were incubated with GST-Gαi3 or GST preloaded with GDP immobilized on glutathione beads. Bound proteins were analyzed by two-color immunoblotting (IB) for GIV CT (His) and pTyr. (**F**) The amount of GTP hydrolyzed in 10

min by His-Gαi3 was determined in the presence of the indicated amounts of sham-treated and in vitro EGFR-phosphorylated His-GIV-CT.

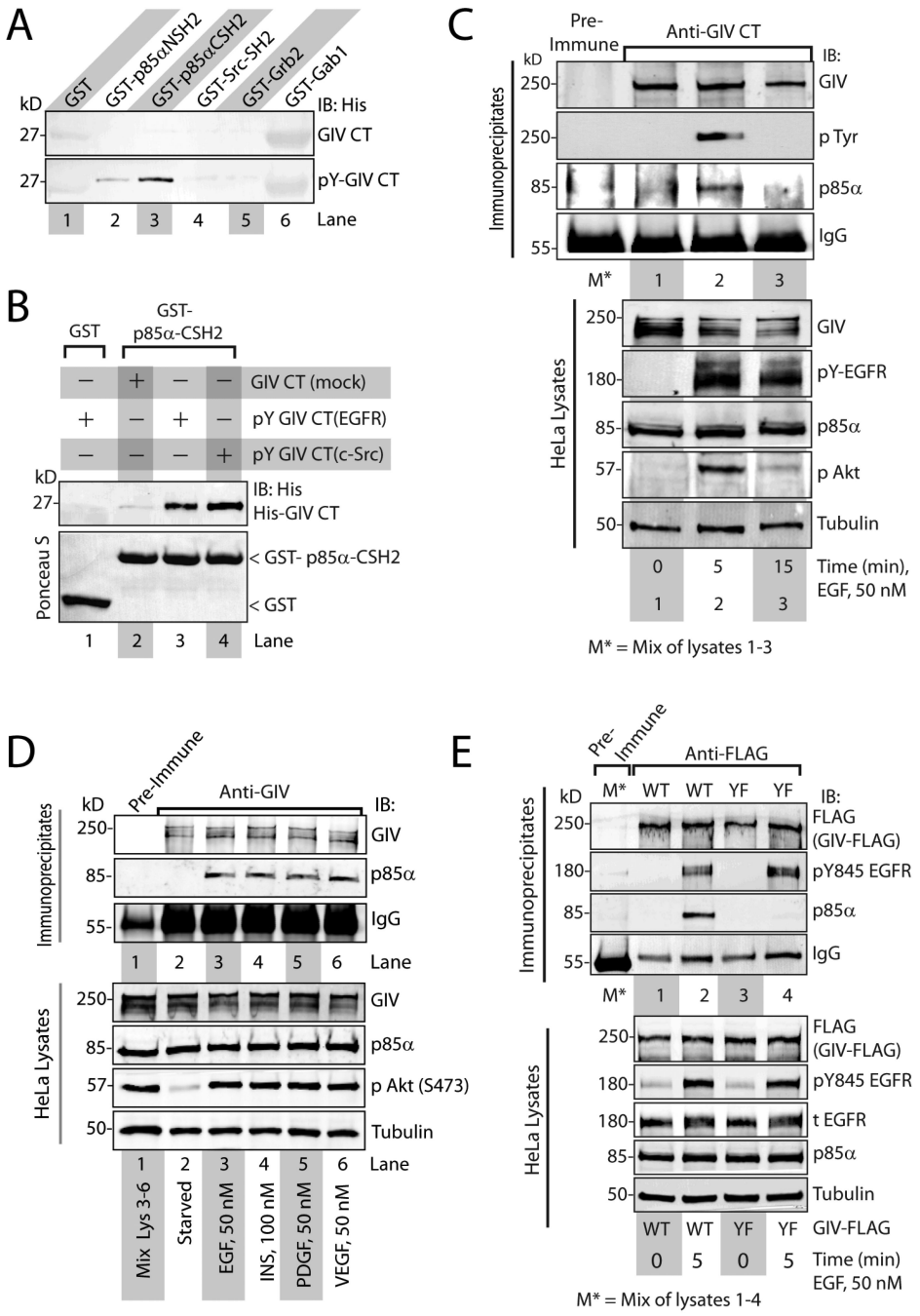

Figure 3. GIV interacts with p85α through its phosphorylated C-terminus

A. Mock-treated and in vitro EGFR-phosphorylated His-GIV-CT were incubated with the indicated GST-tagged SH2 domains or GST immobilized on glutathione beads. Bound His-GIV-CT was analyzed by immunoblotting (IB). **B.** Mock-treated His-GIV-CT and in vitro EGFR or Src-phosphorylated (pY GIV-CT) His-GIV-CT were incubated with GST-tagged C-terminal SH2 domain of p85α (GST-p85α-CSH2) or GST immobilized on glutathione beads. Bound His-GIV CT was analyzed by immunoblotting (IB) with anti-His mAb. **C.** Serum-starved HeLa cells were stimulated with EGF for the indicated time periods. GIV

immuoprecipitates were immunoblotted for endogenous GIV, phosphotyrosine (pTyr) and p85α. **D.** Serum-starved HeLa cells were treated with the indicated growth factors. Immunoprecipitated complexes (top) were analyzed for GIV and p85α by immunoblotting (IB). **E.** Serum-starved Cos7 cells expressing either FLAG tagged-wild-type (WT, lanes 1 and 2) or the phosphotyrosine Y1764,Y1798F mutant (YF, lane 3) were stimulated with EGF. FLAG immune complexes (top) were immunoblotted for GIV-FLAG, ligand-activated EGFR ($pTyr^{845}$ EGFR) and p85α.

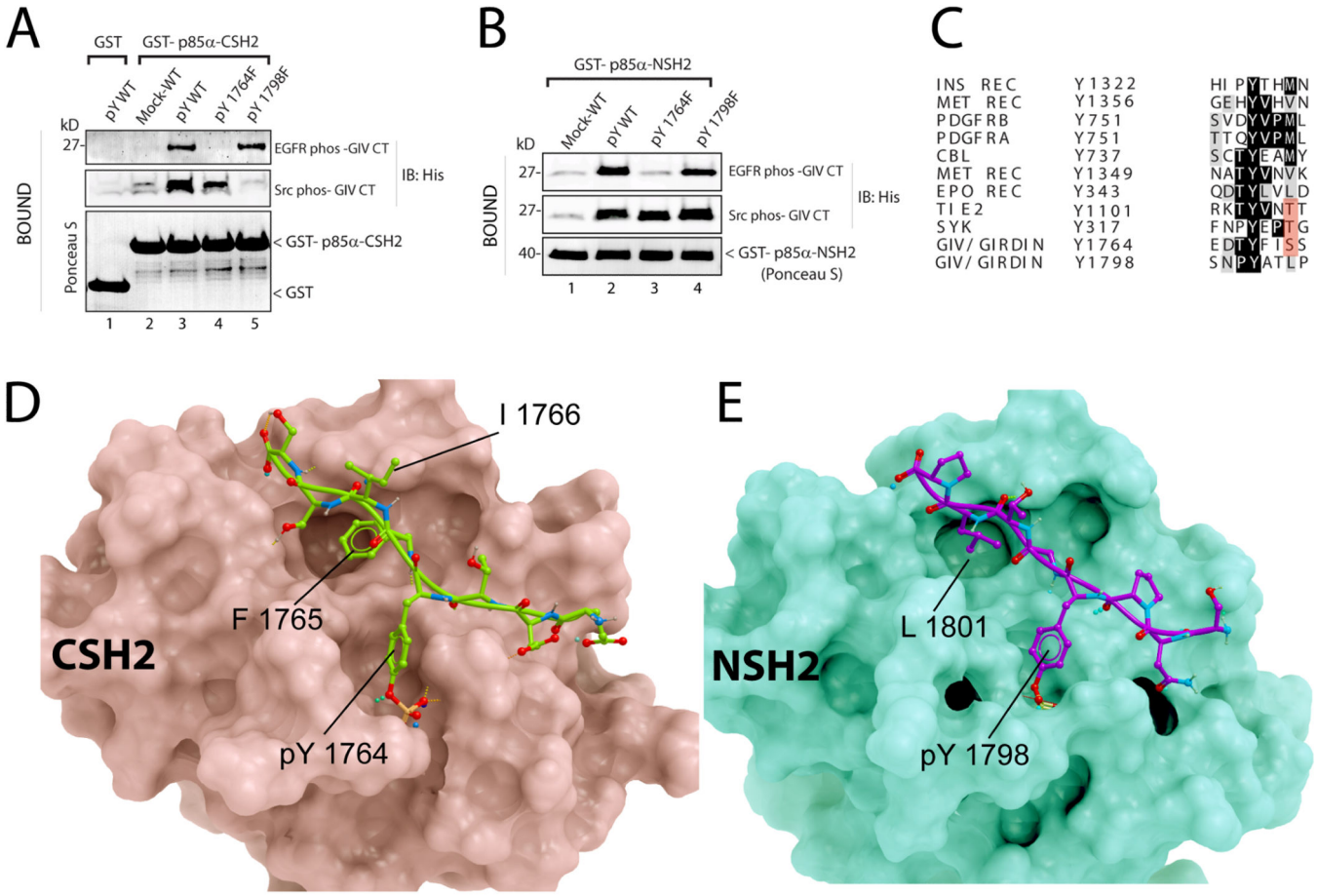

Figure 4. Structural basis for the GIV-p85α interaction

A. His-GIV CT wild-type (pY-WT) and single tyrosine mutants (pY1764F and pY1798F) were phosphorylated in vitro with recombinant EGFR or Src and used in pulldown assays with GST-p85α-CSH2 or GST immobilized on glutathione beads. Bound proteins were immunoblotted for His-GIV CT. **B.** In vitro phosphorylated His-GIV CT wild-type (pY-WT) and single tyrosine mutants (pY1764F and pY1798F) were used in pulldown assays with GST-tagged N-terminal SH2 domain of p85α (GST-p85α-NSH2). **C.** The sequence flanking Tyr^{1764} in GIV was aligned with phosphopeptide-binding sites on other p85α-interacting proteins. **D, E.** Proposed structures of complexes between the C-terminal SH2 domain of p85α (D, pink) and GIV-derived phosphopeptide EDTpY^{1764}FISS (D, green), and between the N-terminal SH2 domain of p85α (E, green) and GIV-derived phosphopeptide SNPpY^{1798}ATLP (E, magenta) are shown. No steric clashes were observed in either model. Detailed views and descriptions of the predicted contacts, **Fig S6**.

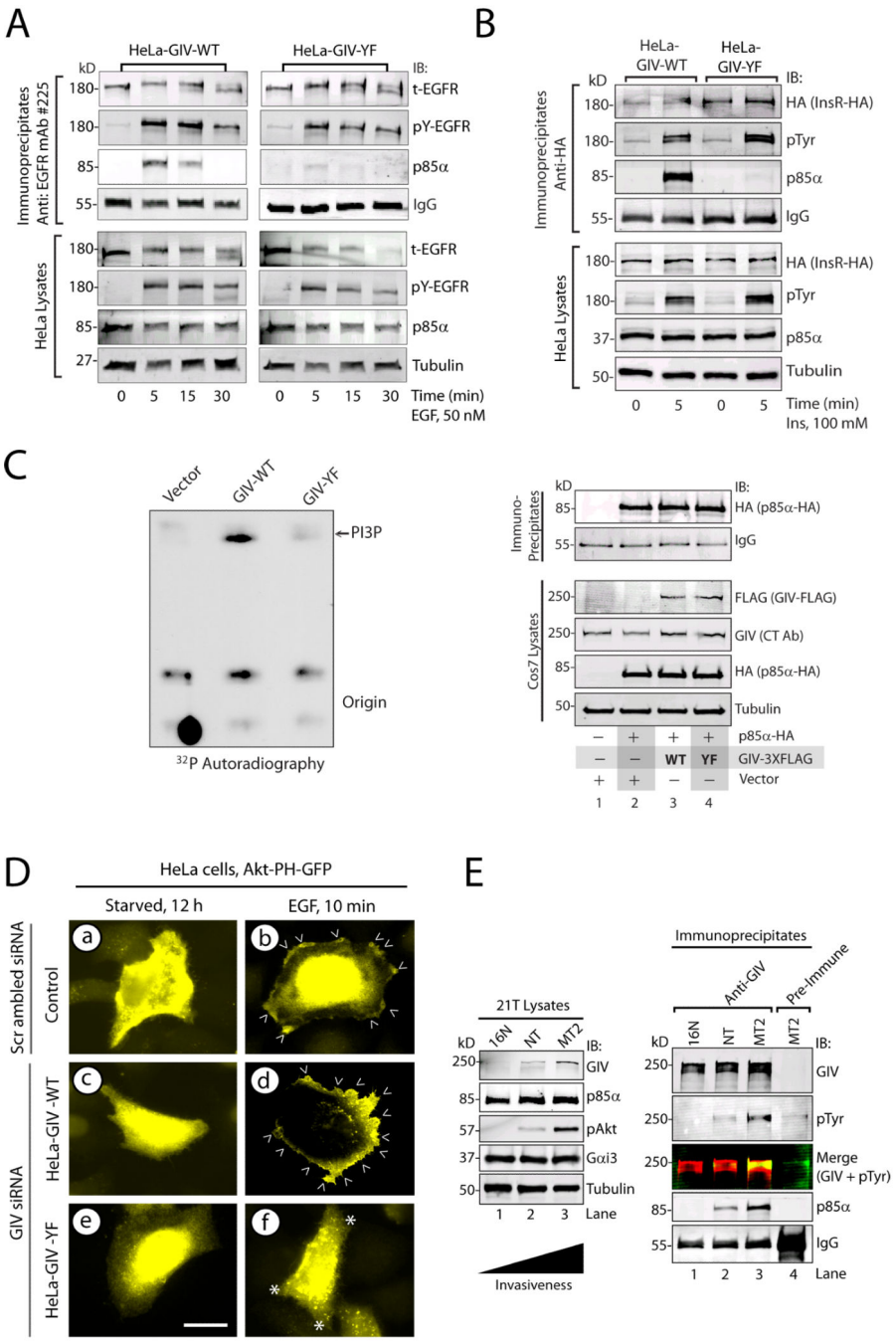

Figure 5. Tyrosine phosphorylation of GIV stabilizes receptor-p85α complexes and increases PI3K activity

A. EGFR immunoprecipitates from serum starved or EGF-stimulated HeLa-GIV-WT and HeLa-GIV-YF cells were immunoblotted for total (t-EGFR) and activated (pY-EGFR) EGFR and p85α. **B.** HA immunoprecipitates (containing HA-tagged insulin receptor; InsR-HA) from serum-starved and insulin-treated HeLa-GIV-WT and HeLa-GIV-YF cells were immunoblotted for HA (to detect InsR-HA), pTyr, and p85α. **C.** Cos7 cells expressing p85α-HA and either wild-type (WT) or phosphotyrosine-mutant (YF) of GIV-FLAG were maintained in 2% FBS for 24 hours. PI3K assays (left) were carried out with

immunoprecipitated p85α-HA, phosphatidylinositol, and [γ-^{32}P] ATP. Lysates and HA immunoprecipitates (containing p85α-HA) were immunoblotted for the indicated proteins (right). **D.** HeLa cells stably expressing either siRNA-resistant wild-type GIV (GIV-WT), phosphotyrosine-mutant GIV (GIV-YF), or vector control were transfected with scrambled or GIV siRNA, then with Akt-PH-GFP plasmid. Cells were serum-starved or treated with EGF, then stained for GFP (yellow) and with DAPI (blue). Bar = 10 μM. **E.** Lysates (left) from 21T series of cells (16N, NT, and MT2) were immunoblotted for GIV, p85α, phospho-Akt (pAkt), Gαi3, and tubulin. GIV immunoprecipitates from lysates (normalized for equal abundance of GIV protein) were analyzed by two-color immunoblotting (IB) for GIV, p85α, and pTyr.

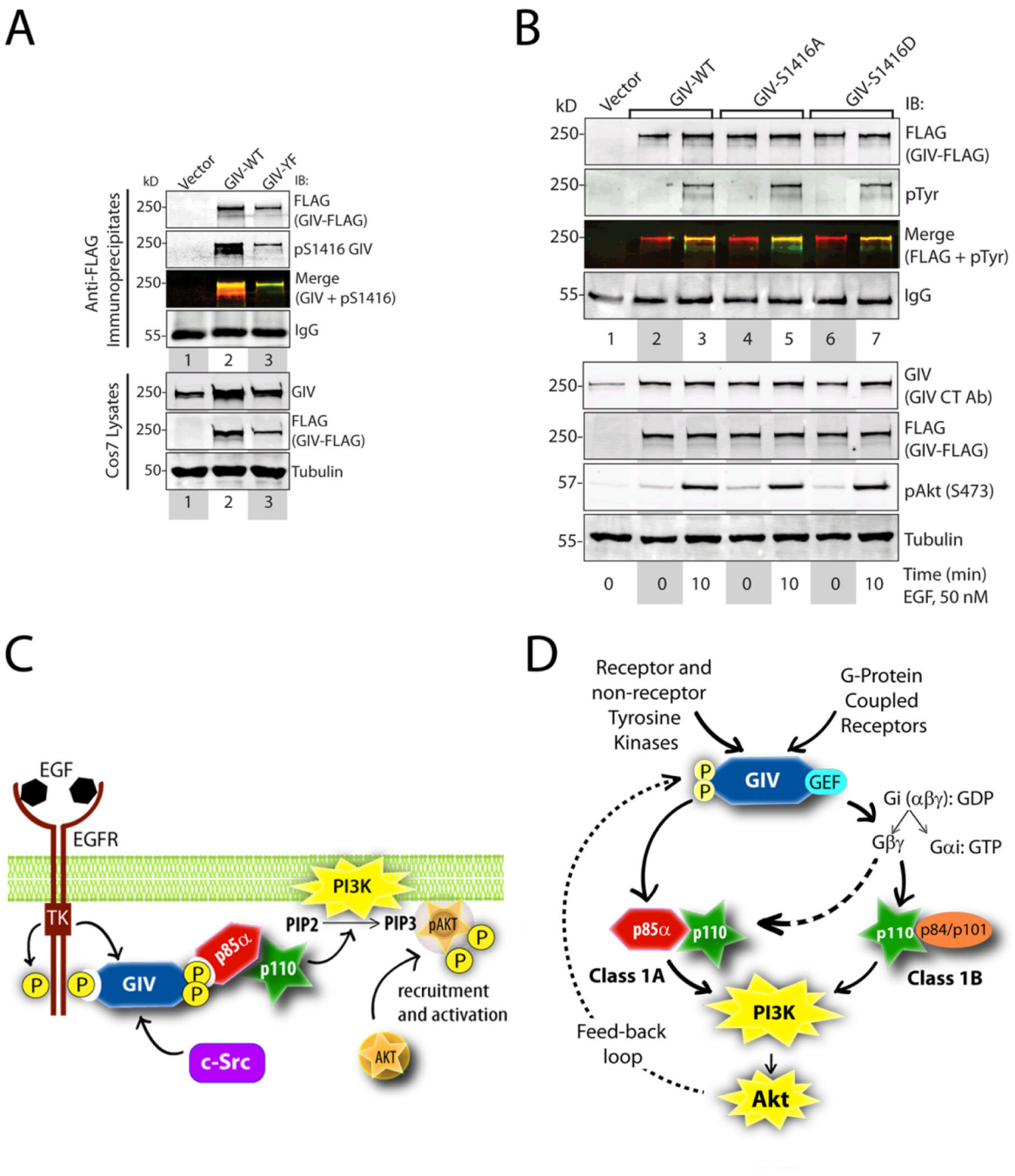

Figure 6. The dual role of GIV as an enhancer of and a substrate for Akt kinase

A. Cos7 cells expressing vector, GIV-WT-FLAG or GIV-YF-FLAG were maintained in the presence of 2% FBS. FLAG immunoprecipitates were analyzed by two-color immunoblotting (IB) for FLAG (to detect GIV) and pSer^{1416} GIV. **B**. Cos7 cells expressing wild-type (GIV-WT-FLAG), or phosphoserine mutants of GIV (GIV-S1416A-FLAG and GIV-S1416D), or vector control were serum starved or stimulated with EGF. FLAG immunoprecipitates were analyzed by two-color immunoblotting (IB) for GIV and pTyr. **C**. Upon ligand stimulation, EGFR is activated and is autophosphorylated. GIV is recruited to

the autophosphorylated cytoplasmic tails of activated receptors. Activated receptor and non-receptor tyrosine kinases (such as c-Src) phosphorylate GIV at two tyrosine residues, which are direct binding sites for the SH2 domains of the regulatory p85α-subunit of PI3K. We propose that GIV stabilizes the receptor-p85α complexes, triggers the activation of PI3K, and augments the production of PIP_3 at the plasma membrane. **D.** Working model for how GIV enhances class 1 PI3K activity. The phosphotyrosines of GIV directly interact with p85α and activate class IA PI3K (solid, left arrow). Akt-dependent phosphorylation of GIV at Ser^{1416} requires GIV-dependent activation of the PI3K-Akt pathway. This implies that tyrosine phosphorylation of GIV occurs upstream of Akt-mediated phosphorylation of GIV; the latter event may set up a feedback loop (interrupted, left arrow). The GEF motif of GIV activates Gi, releases free Gβγ-subunits, which in turn directly interact and activate the catalytic p110γ-subunits of class 1B PI3Ks (solid, right arrow)(62). The Gβγ-pathway can also bind and activate the catalytic p110β subunits of class 1A PI3Ks (interrupted, right arrow)(61). Thus, the GIV-mediated direct and indirect enhancement of class 1 PI3K activity may synergistically amplify PI3K activity at the plasma membrane.